Climate Change and Density Dependence in the North Pacific: Applications to Salmon Run Forecasting and Plankton Population Dynamics

Grant Woodard

A thesis

submitted in partial fulfillment

of the requirements for the degree of

Master of Science

University of Washington

2023

Committee:

Daniel Schindler

Ray Hilborn

Jan Ohlberger

Program Authorized to Offer Degree:

School of Aquatic and Fishery Sciences

University of Washington

Abstract

Climate Change and Density Dependence in the North Pacific: Applications to Salmon Run Forecasting and Plankton Population Dynamics

Grant Woodard

Chair of the Supervisory Committee:

Daniel Schindler

School of Aquatic and Fishery Sciences

We explore the role of density dependence and climate change in impacting different trophic levels of the North Pacific Ocean which supports some of the world's largest fisheries. First, we evaluated the use of density dependent growth in autoregressive models to improve forecasting methodology for Sockeye Salmon in Bristol Bay, Alaska. Bristol Bay supports the world's largest fishery for sockeye salmon which are harvested during an extremely condensed time period as fish return to their natal rivers. Uncertainties in pre-season forecasts of run size challenge managers and the fishing community because of limited time to adapt management, fishing, and processing strategies within a season. Pre-season forecasts between 2005 and 2022 were off by as much as 29%, with a mean absolute percent error of 16%. We found that autoregressive models including mean length-at-age of returning sockeye salmon as well as

previous year's run size, summer sea surface temperature, and competitor abundance (i.e., pink salmon) produced accurate predictions of run size for sockeye salmon substantially earlier in the season than is currently possible via pre-season or current in-season methods. Our best model had an average mean absolute percent error between observed and predicted run sizes on June 24th of 12%, a level of error not met by current in-season methods until July 11th and better than current pre-season methods in the majority of years. This provides valuable management benefits to managers and the fishing industry.

Next, we evaluated the potential role of climate change in shaping zooplankton population biomass and size structure as zooplankton provide an important food source for all Alaskan fisheries. Climate change is warming the earth and its oceans, and these trends are expected to continue for the next century. These temperature changes could have major ecosystem impacts starting at the lower trophic levels such as zooplankton and cascading up the system, potentially due to changes in zooplankton size structure with increasing temperatures. Thus, we seek to assess impacts to zooplankton population demographics in the Bering Sea using a physiologically structured population model consisting of a semi chemostat phytoplankton resource and a zooplankton consumer divided into a juvenile and adult stage. Our model predicts that increased temperatures will lead to increased extinction risk starting at around 15 C, but that decreases in size at maturity down to approximately 62 μg would allow the population to persist at higher temperatures. However, this has the added consequence of a decreased size structure of the population. Such a collapse of the forage base or decrease in size structure could have cascading impacts to the rest of the ecosystem including reductions in carrying capacity and size at age of important fish species.

TABLE OF CONTENTS

ACKNOWLEDGEMENTS

We thank the Alaska Department of Fish and Game, particularly Bert Lewis and Stacy Vega for providing data and for feedback on the approach for developing the models. Sockeye salmon abundance and size at age data analyzed during this study are available from the Alaska Department of Fish and Game upon reasonable request. Pink Salmon abundance data is available from Greg Ruggerone upon request. Sea Surface Temperature is available from the NOAA Physical Sciences Laboratory's NCEP/NCAR Reanalysis monthly mean SST dataset. Funding for the salmon forecasting study was provided through a fellowship to GW from the University of Washington, School of Aquatic and Fishery Sciences.

We also thank the National Oceanic and Atmospheric Administration, particularly David Kimmel, for providing data and feedback on the zooplankton modeling approach. The *Calanus* sample data used in this study is available from NOAA upon reasonable request. We also express gratitude towards Max Lindmark for his immense help with model design, implementation, and troubleshooting. The authors declare there are no competing interests.

Chapter 1. BODY SIZE AS A LEADING INDICATOR OF RUN SIZE AND APPLICATION TO IN-SEASON FORECASTING OF SOCKEYE SALMON IN BRISTOL BAY, ALASKA

Authors: Grant A. Woodard[1*], Daniel E. Schindler[1], Jan Ohlberger[1,2], and Curry Cunningham[3]

[1]School of Aquatic and Fishery Sciences, University of Washington, Seattle, WA 98195, USA

[2] Washington Department of Fish and Wildlife, 1111 Washington St. SE, Olympia, WA 98501, USA

[3]University of Alaska Fairbanks, Fairbanks, AK 99775, USA

*Correspondence: Email: gwooda@UW.edu

1.1 ABSTRACT

Bristol Bay supports the world's largest fishery for sockeye salmon which are harvested during an extremely condensed time period as fish return to their natal rivers. Uncertainties in pre-season forecasts of run size challenge managers and the fishing community because of limited time to adapt management, fishing, and processing strategies within a season. Pre-season forecasts between 2005 and 2022 were off by as much as 29%, with a mean absolute percent error of 16%. We found that autoregressive models including mean length-at-age of returning sockeye salmon as well as previous year's run size, summer sea surface temperature, and competitor abundance (i.e., pink salmon) produced accurate predictions of run size for sockeye salmon substantially earlier in the season than is currently possible via pre-season or current in-season methods. Our best model had an average mean absolute percent error between observed

and predicted run sizes on June 24th of 12%, a level of error not met by current in-season methods until July 11th and better than current pre-season methods in the majority of years. This provides valuable management benefits to managers and the fishing industry.

1.2 INTRODUCTION

Forecasting models are used extensively in fisheries to predict population abundance to inform decisions for setting harvest limits and adapting fishing strategies. In the case of salmon fisheries, this often takes the form of an advanced pre-season forecast (e.g., several months prior) that is then refined with in-season forecasts as data on run size become available during the fishery (e.g., Staton and Catalano 2018). In a perfect world with high quality data and deep understanding of ecosystems, mechanistic models based on fish biology and ecology could be developed to predict population size for informing sustainable fishing rates (Ward et al. 2014). Instead, simple time-series models of abiotic and biotic variables that correlate with measures of interest (e.g., run size, fish size) often perform better than more complex models (Adkison and Peterman 2000; Ward et al. 2014). Such time-series models can provide information on run size and timing to fishery managers and the fishing industry to improve their in-season decisions.

Bristol Bay, Alaska, supports the world's largest sockeye salmon (*Oncorhynchus nerka*) fishery, producing over half the annual catch of this species from the North Pacific Ocean on average (Ruggerone et al. 2010). Most fish harvested spend either 2 or 3 years in the ocean, which we will refer to as ocean age-2 and ocean age-3, respectively, before returning to spawn in

their natal rivers. Since a period of low productivity that ended in the mid-1970s, Bristol Bay has seen large returns of sockeye salmon including record returns in the last decade (Tiernan et al. 2021). Bristol Bay sockeye salmon are harvested during their migration back to rivers during a condensed commercial fishing season that primarily lasts from late June to the end of July (Dann et al. 2013). The short season provides a time sensitive opportunity to adjust management or fishing strategies in-season thereby making early season indicators of run size particularly valuable to managers and the fishing industry.

Management of Bristol Bay sockeye salmon is currently separated into five fishing districts, each of which is regulated by a manager who makes daily decisions about when to open set and drift gillnet fisheries. The fishery is managed with escapement goals for each river, where managers are required to allow a certain number of fish to reach the spawning grounds. Accurate pre-season and in-season forecasts aid managers because they help clarify how aggressively to allow harvest at the beginning of the fishing season. Without reliable forecasts managers might be inclined to harvest conservatively at the beginning of the season, thereby producing missed harvest opportunities during years with large returns. In contrast, during years of low returns, managers run the risk of not achieving their escapement goal if they harvest too aggressively early in the season.

The current cycle of run forecasting for Bristol Bay sockeye salmon is used by both managers and the fishing industry. Pre-season forecasts are made every fall (~ November) to predict how many fish will return to each of the rivers in Bristol Bay the following summer

(June-August). The processing industry uses these forecasts to make logistical and hiring decisions that impact their business. Once the fishery starts in late-June, managers gain information about the number of fish returning by the catch and escapement data as it accumulates and fish size from samples of the catch and escapement. Additional information on returning fish age and size, run timing, and stock of origin is available from the Port Moller test fishery (Dann et al. 2013). This in-season information is used to adjust the pre-season forecast as the summer progresses in response to in-season indicators such as the accumulating catch and escapement, and the catch rates in the Port Moller test fishery (Adkison and Peterman 2000; Fried and Hilborn 1988; Hyun et al. 2005; Link and Peterman 1998; Su, and Adkison. 2002). However, using current methods (which do not incorporate the available data on fish size), in-season run size adjustments are not very informative until well into July, at which point the fishery is often beginning to wind down.

There is a negative correlation between the body size of adult sockeye salmon and the number of returning fish, which is a result of density dependent growth in the ocean (Rogers and Ruggerone 1993; Ohlberger et al. 2023). Here we explored whether this relationship, in combination with other abiotic and biotic factors that affect growth of Bristol Bay sockeye salmon, can be used to predict run size several weeks earlier during the fishing season than is currently possible. Other variables include the abundance of pink salmon (*Oncorhynchus gorbuscha*) that compete with Bristol Bay sockeye salmon and ocean sea surface temperatures which emerged as major drivers of sockeye growth in a recent retrospective analysis of changes

in body size of Bristol Bay sockeye salmon (Ohlberger et al. 2023). We then compare whether our predictive models outperform current pre-season and in-season Bristol Bay sockeye salmon forecasting methodology.

1.3 METHODS

We quantified whether the relationship between sockeye adult size-at-age and the run size to Bristol Bay can be used to accurately predict sockeye run size during the fishing season. The data consists of length-at-age measurements of sockeye salmon collected by in-river sampling with beach seines and gill nets by the Alaska Department of Fish and Game (ADF&G), and from fish sampled from commercial catches. Fish size was determined as body length (mid-eye to fork to nearest mm) and ages were determined from scale pattern analysis (Tobias et al. 1994). We additionally used data from the Port Moller test fishery operated by the Bristol Bay Science and Research Institute (BBSRI) beginning on June 10 each year, but smaller sample sizes may limit its ability to provide earlier in season information before the first commercial fishery and in-river sampling data are also available. Size-at-age data and total run sizes used in the analyses were collected by ADF&G between 1980 and 2022. Additional data for environmental variables that potentially affect sockeye run size such as North Pacific sea surface temperatures and North Pacific pink salmon abundances in the previous year (Ohlberger et al. 2023) were considered as covariates in forecasting models. North Pacific pink salmon abundance was found to exert a large influence on model predictions in extreme years. Therefore, given that dominant pink

salmon runs occur in alternating years, we explored using whether the year was odd or even as a covariate to implicitly account for the role of pink salmon on sockeye salmon growth. Data was available for these variables for several decades prior to the 1980s but we have elected to truncate the data at 1980 (1979 for auto-regressive variables) because of the new productivity regime that appeared in Bristol Bay in the mid-1970s (Mantua et al. 1997).

We developed auto-regressive time-series models that quantify relationships between sockeye run size and in-season size-at-age, along with pink salmon abundance in the North Pacific Ocean in the previous year, odd or even year, and previous mean summer and winter sea surface temperatures. We then used one step ahead forecasts to assess model performance. These analyses were performed over a range of dates in the season (late June and early July) to assess how early in the fishing season the models can be effectively used to predict annual sockeye run size. Multiple versions of these models were tested using data on fish that spend either 2 or 3 years in the ocean which compose the vast majority of returning Bristol Bay sockeye (Ohlberger et al. 2023).

The full model takes the general form:

$$\boldsymbol{R_t = R_{t-1} + S_{t,d} + T_{t-1} + P_{t-1} + \varepsilon}$$

Where:

$\boldsymbol{R_t}$ is the Bristol Bay sockeye salmon run size for the year (t) we are predicting,

$\boldsymbol{R_{t-1}}$ is the previous year's sockeye salmon run size,

$\boldsymbol{S_{t,d}}$ is the observation of average fish size for a given age (either ocean age-2 or ocean age-3 fish) up to a specific day (d) in the season,

$\boldsymbol{T_{t-1}}$ is the sea surface temperature in Bristol Bay in the previous summer or winter. Mean monthly Bristol Bay sea surface temperature data was obtained from the NOAA Physical Sciences Laboratory's NCEP/NCAR Reanalysis monthly means SST dataset,

$\boldsymbol{P_{t-1}}$ is last year's abundance of pink salmon in the North Pacific Ocean. This variable was considered either as a continuous measure of pink salmon abundance, or as a categorical value to account for whether it was an odd or even year as a simple surrogate for a pink salmon effect given their regular 2-year cycle of abundance (Ruggerone and Irvine 2018), and $\boldsymbol{\varepsilon}$ is random normal error.

We fit multiple alternative models (Table 1.1) that include different subsets of the variables described above to determine which models performed best for making in-season forecasts of total run size over the last 18 years (2005 to 2022). Models were fit retrospectively

to data from 1979 to 2004. From 2005 to 2022 'in-season' forecasts were generated as the model was updated iteratively one year at a time. Model parameters were estimated using least squares linear regression analysis in R assuming normally distributed random errors (R Core Team 2023). Forecast performance was evaluated by identifying the models with the lowest mean absolute percent error (MAPE) between the predicted and observed total run size across the 18 test years.

We also wanted to assess if a weighted prediction using multiple model formulations (also known as ensemble modelling) would improve model accuracy. We opted to use an inverse variance approach. In this approach, we used model predictions and observations from 2005 to 2009 to obtain an initial ranking of model performance by their MAPEs. For each year from 2010 to 2022, the top 5 models were identified by selecting the 5 models with the lowest MAPE. For each of these top 5 models, the inverse variance was calculated from the weighted predictions for the years prior to the test year back to 2005. Test years started in 2010 and proceeded iteratively to 2022. These inverse variances were scaled to the sum of the inverse variances for these top 5 models for each test year and multiplied by the prediction for the corresponding top 5 models, generating a weighted prediction for each model for each test year based on the observed and predicted run sizes from 2005 to the year before the test year. These weighted predictions from each model in each year were then summed to obtain a weighted prediction of total run size in each year.

In addition to comparing the unweighted model performance to a weighed prediction, our in-season forecast performance was also compared to the performance of pre-season models based on sibling-return models (Ovando et al. 2022) which are virtually independent of one another.

For a direct evaluation of in-season forecast model performance, we compare the mean absolute percent error (2010-2022) of one-step ahead predictions from the size-at-age model with that of an existing in-season forecast model for Bristol Bay sockeye salmon. This existing in-season forecast model uses Bayesian methods to update the annual pre-season forecasts when fit to catch per unit effort and age composition data from the Port Moller Test Fishery and fishing district-specific inshore catch and escapement data by date (Cunningham, unpublished). Run size predictions derived from both in-season forecast methods were generated every second day across the commercial fishing season (June 16 - July 16) for each year 2005-2022, based on the fitted relationship from the prior year (i.e. one-step ahead). These every other day predictions for each year were compared with the observed run size in each year, and the mean absolute percent error for each day across the season was calculated for each forecast model type.

1.4 RESULTS

There were strong negative correlations between the size-at-age for ocean age-2 and ocean age-3 fish and the total return of sockeye salmon to Bristol Bay between 1980 and 2022 (Figure 1.1 A, B). The interannual range in observed mean length was approximately 50mm for

both age classes. The mean absolute percent difference between the estimated mean size-at-age during the season and the value measured at the end of the season declined over the course of the season and by late June was approximately 1% (Figure 1.1 C, D); thus, the annual aggregate estimates of size-at-age could be estimated accurately based on data collected through June 24th, the date for which all following metrics of model success are calculated.

The best performing model using ocean-age-2 fish included size-at-age, the sockeye run size in the previous year, and the mean summer sea surface temperature in the previous year (Figure 1. 2 A; Table 1.2, 1.3). This model had a MAPE of 12% based on average comparisons between observed run size and one step ahead predictions between 2005 and 2022 (henceforth referred to as $MAPE_{2005\text{-}2022}$). The adjusted R^2 for this model's iterative retrospective fits (ending from 2004 to 2021 and henceforth labeled $R^2_{2004\text{-}2021}$ and not to be confused with metrics measuring one step ahead prediction performance like MAPE) averaged 18.5% reaching 40.9% in 2021. For this model's retrospective fit, 17.7% of the $R^2_{2004\text{-}2021}$ was explained by size-at-age, 74.5% was explained by the previous year's sockeye return, and 7.6 % was explained by the mean sea surface temperature during the previous summer. The best performing model using ocean-age-3 fish for predicting the run size of sockeye salmon returning to Bristol Bay included size-at-age, the sockeye run size in the previous year, the mean summer sea surface temperature in the previous year, and pink salmon abundance in the previous year (Figure 1.2 B; Table 1.2, 1.3). This model had a $MAPE_{2005\text{-}2022}$ of 14%. The $R^2_{2004\text{-}2021}$ for this model's retrospective fits averaged 27.5% reaching 50.4% in 2021. On average, 45.7% of the $R^2_{2004\text{-}2021}$ was explained by

size-at-age, 34.5% explained by the previous year's sockeye return, 14.8% explained by the pink salmon abundance in the previous year, and 4.8% explained by the previous summer's mean sea surface temperature. Correlations between observed run size and one step ahead predictions for both models are quite high (0.87 for ocean age-2 and 0.83 for ocean-age 3; Figure 1.2 C, D, E; Table 1.2). Coefficients for these two on average best performing models as used to predict the sockeye return in 2023 are presented in table 1.3. Reported MAPE for the weighted model (and in turn the reported correlation between observed run and the weighted model prediction) was calculated over 2010-2022 to allow for a 5 year period between 2005 and 2009 to obtain starting MAPE values to identify the order of model performance when weighting models in 2010. The weighted prediction across all models had a $MAPE_{2010\text{-}2022}$ of 15 %, meaning it performed moderately well but not as well as the individual best performing models.

In 2022, the total sockeye salmon return to Bristol Bay was 83 million fish, 12 million above the previous record observed 71 million fish and 11 million over the 2022 pre-season forecast of approximately 72 million fish. This provided a unique opportunity to assess the performance of the model in forecasting an extreme value. Our best models on average (model 7, using ocean age-2 size-at-age, and model 5, using ocean age-3 size-at-age) predicted a return of approximately 63 and 60 million sockeye salmon respectively in 2022. Thus, although the size-at-age models under-forecasted the observed record return, they did succeed in indicating that the run would be among the largest on record by the last week of June. The best performing models (model 7 using ocean age-2 length-at-age data and model 5 using ocean age-3 length-at-age data)

both outperformed the pre-season forecast in 11 of the 18 test years between 2005 and 2022, indicating that our models tend to be slightly more accurate than the pre-season forecast (Figure 1.2 F).

Comparison of MAPE for forecasts based on size at ocean age 2 (Model 7) and ocean age 3 (Model 5), with the existing Bayesian integrated in-season forecast model (Figure 1.3), indicate that both size-at-age models exhibit lower average error rates until just past the average peak in the Bristol Bay season ~July 10th. After this point the Bayesian integrated in-season forecast approach (Cunningham, unpublished; Fried and Hilborn 1988; Hyun et al. 2005) shows a reduced error rate as the fishing season finishes.

1.5 DISCUSSION

Because of density dependent growth in the ocean there is a strong relationship between the body size of sockeye salmon and the number of fish that return to Bristol Bay (Rogers and Ruggerone 1993; Ohlberger et al. 2023). This relationship formed the core of our in-season model as reliable estimates of body sizes are obtainable by late June and can be used as a leading indicator of total sockeye run size in Bristol Bay. Our analyses also considered several environmental covariates that have the potential to affect the growth and survival of sockeye salmon and, therefore, modify the relationship between body size and run size. Pink salmon abundance has a negative impact on sockeye salmon growth through competition for food (Ruggerone et al. 2010), and summer sea surface temperature exerts a negative influence on

sockeye salmon growth, while winter sea surface temperature exerts a positive influence on sockeye salmon growth (Ohlberger et al. 2023). Our best performing forecast models in terms of MAPE included size-at-age, the sockeye run size in the previous year, and the previous summer sea surface temperature, with and without pink salmon abundance in the previous year (for ocean age-2 and ocean age-3 fish respectively).

Our models are useful for several reasons. First, size-at-age is a simple metric to measure with low error, so accurate estimations of size-at-age are easy to make in-season. Additionally, size-at-age integrates across many different ecological factors that affect the ecology of Bristol Bay sockeye salmon during their ocean residency. Third, we focused our model on the scale of Bristol Bay which accounts for about half of the sockeye salmon abundance in the North Pacific Ocean. We expect that size-at-age is not likely to be as effective for smaller stocks or for predicting sockeye runs to individual rivers.

Our best model in terms of MAPE underpredicted the record high 2022 run of Bristol Bay sockeye salmon by about 23.8 % while the weighted model underpredicted the run by about 24.3 %; however, our best models still predicted that one of the largest returns would be observed which would have had utility for both managers and the fishing industry. Not only were our models able to predict large and small runs, but they were able to do so by June 24th which is substantially earlier in the fishing season than currently used approaches arrive at a reliable assessment of run size. These results emphasize the importance of early-season sampling if our approach is adopted for improving in-season interpretation of how the run is developing.

Our best in-season forecast models included size-at-age, sockeye return in the previous year, and mean summer sea surface temperature in the previous year. These variables are largely independent of the data used to generate pre-season forecasts (Ovando et al. 2022) and provide an objective confirmation of the pre-season forecast early in the fishing season. Thus, our study would allow managers to forecast runs both more accurately and earlier in the season to adjust harvest management accordingly. Benefits would also accrue to the fishing industry who could adjust logistical and staffing decisions accordingly based on their confidence about the size of the run they could expect in any given year. This methodology could be used in other important fisheries and salmon systems (provided they have high enough abundance to generate density-dependent growth) to predict run size more accurately. The key will be to determine the appropriate spatial scales to assess the relationship between salmon abundance and growth rates.

1.6 TABLES

Table 1.1. A summary of covariates included in each of the model variations.

The 13 model variants tested for ocean age-2 and ocean age-3 fish, respectively. Models 11, 12 and 13 do not use sockeye size-at-age data and instead use only environmental covariates or previous sockeye return. The bold models (5 and 7) were the best performing models for ocean age-3 and ocean age-2 fish respectively.

Model	Size-at-age (mm)	Sockeye run (t-1) (thousands)	Previous Summer SST	Previous Winter SST	Odd or Even Year	Pink Salmon Abundance (millions) (t-1)
1	X					
2	X	X				
3	X	X				X
4	X	X			X	
5	**X**	**X**	**X**			**X**
6	X	X	X		X	
7	**X**	**X**	**X**			
8	X	X		X		X
9	X	X		X	X	
10	X	X		X		
11		X	X	X		X
12		X	X	X	X	
13		X				

Table 1.2. A summary of model performance metrics.

Presented are the mean absolute proportion of error (MAPE), maximum absolute proportion of error, standard deviations of the absolute proportion of error, and correlations for each of the 23 model variants on June 24th. Bold models were the best for each age group. Models 11-13 do not include size-at-age as a predictor.

Age	Model	Mean Error	Max Error	SD Error	Correlation
2	1	0.16	0.55	0.15	0.80
2	2	0.13	0.42	0.11	0.88
2	3	0.13	0.42	0.10	0.89
2	4	0.13	0.52	0.13	0.86
2	5	0.13	0.35	0.09	0.87
2	6	0.13	0.42	0.11	0.85
2	**7**	**0.12**	**0.32**	**0.09**	**0.87**
2	8	0.18	0.43	0.12	0.78
2	9	0.19	0.54	0.15	0.73
2	10	0.18	0.49	0.14	0.73
3	1	0.18	0.67	0.17	0.78
3	2	0.16	0.52	0.12	0.86
3	3	0.14	0.58	0.14	0.85
3	4	0.18	0.64	0.14	0.86
3	**5**	**0.14**	**0.48**	**0.12**	**0.83**
3	6	0.17	0.54	0.13	0.84
3	7	0.15	0.43	0.11	0.85
3	8	0.16	0.55	0.14	0.81
3	9	0.19	0.62	0.16	0.79
3	10	0.17	0.49	0.14	0.80
NA	11	0.19	0.43	0.12	0.65
NA	12	0.19	0.38	0.12	0.61
NA	13	0.16	0.38	0.12	0.86
All	Weighted	0.15	0.42	0.12	0.87

Table 1.3. Model coefficients for the best two models as used to predict run size in 2023.

Coefficients for the best performing models for each age group when including all data from 1979 to 2022 (used to predict the 2023 run size in thousands). This model included mean size-at-age (mm), sockeye run size in the previous year (thousands), and mean summer sea surface temperature (°C) in the previous year for ocean age-2 fish, and these same variables with the addition of pink salmon abundance in the previous year (millions) for ocean age-3 fish.

Ocean Age	Model	Intercept (SE)	Length-at-age (SE)	Previous Return (SE)	Previous SST (SE)	Previous Pink Salmon Abundance (SE)
2	7	183300 (96390)	-357.3 (173.2)	0.54 (0.13)	1774 (1720)	NA
3	5	397100 (123200)	-663.3 (197.3)	.42 (.13)	1197 (1594)	-22.8 (15.3)

1.7 FIGURES

Figure 1.1. Relationship between observed run size and average length at age and mean absolute percent difference between mean observed size-at-age on a given day and mean observed size-at-age at the end of the season.

Relationship between sockeye salmon run size to Bristol Bay (in millions) between 1980 and 2022 and the average length of ocean age-2 and ocean age-3 fish respectively (A, B). Mean absolute percent difference between mean observed size-at-age on a given day and mean observed size-at-age at the end of the season (C, D).

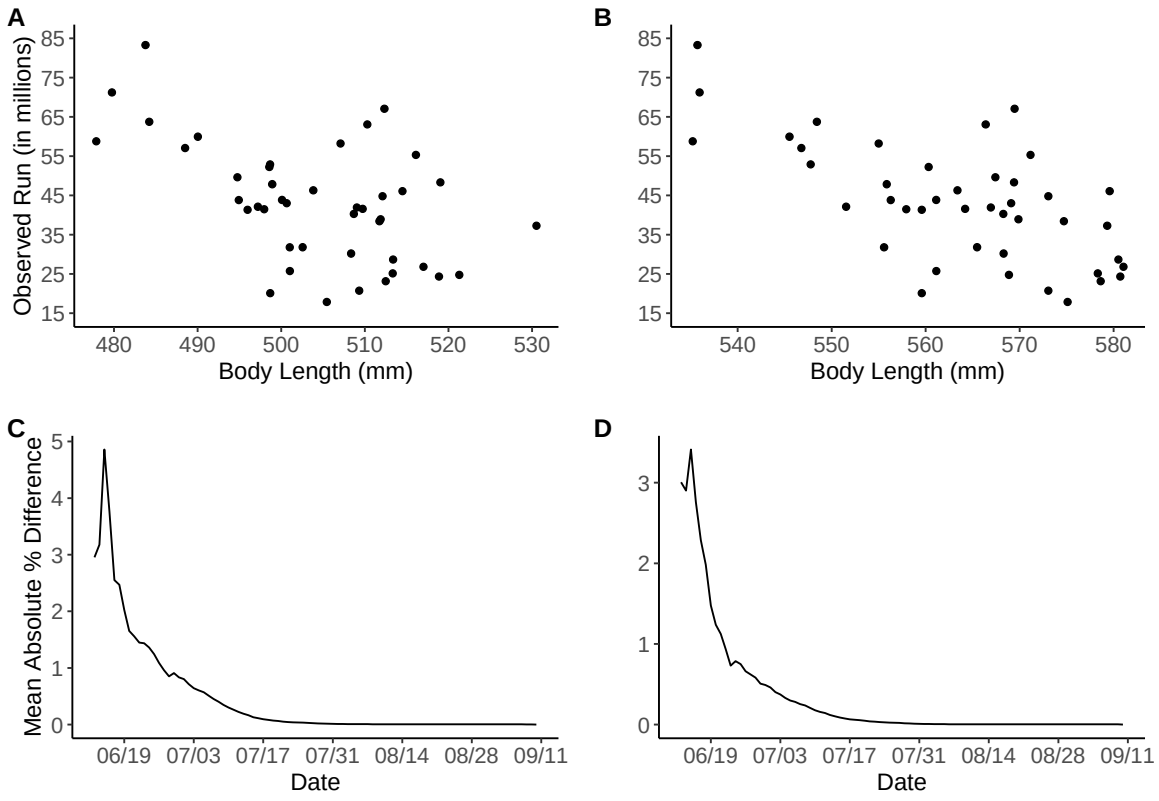

Figure 1.2. Graphs of model retrospective and prospective fits, correlations between model observations and predictions, and comparisons of preseason forecasts and model predictions.

Retrospective fit (left of the vertical line) and prospective model predictions based on ocean age-2 (A) and ocean age-3 (B) fish respectively from one step ahead forecasts made on June 24th. Models presented are the best performing models on average for ocean age-2 and ocean age-3 fish respectively (model 7, blue and model 5, red). The black line is the best performing model in 2022 (model 2 for both ages). Black dots are the total sockeye run in that year. Correlation between observed total run size and predicted total run size based on data available at that time for the best performing models (model 7 and model 5 from 2005 to 2022) for ocean age-2 fish (C) and ocean age-3 fish (D) respectively, and the weighted average prediction from 2010 to 2022 (E). Diagonals are 1:1 lines. (F) Pre-season forecasts from sibling return models (Ovando et al. 2022; filled circles) and in-season predictions of run size from the two best performing models (red and purple open circles) along with observed run size (grey bars) from 2010 to 2022.

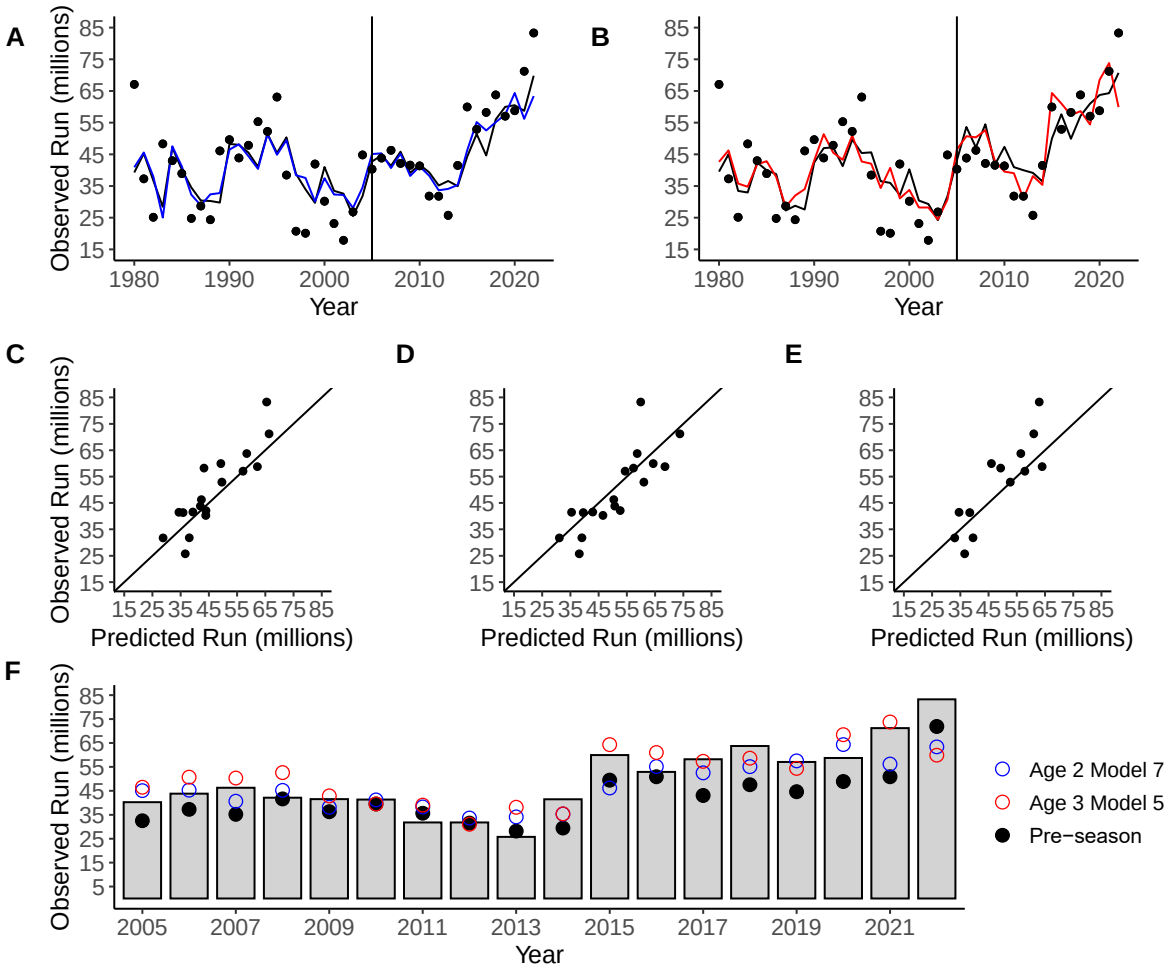
A
B
C
D
E
F
Observed Run (millions)
Year
Predicted Run (millions)
Age 2 Model 7
Age 3 Model 5
Pre−season

Figure 1.3. Mean absolute percent error of best models over the course of the season compared to current in-season forecast methodology.

Mean absolute percent error (MAPE) over the course of the season for models 5 and 7 compared to current in-season methodology.

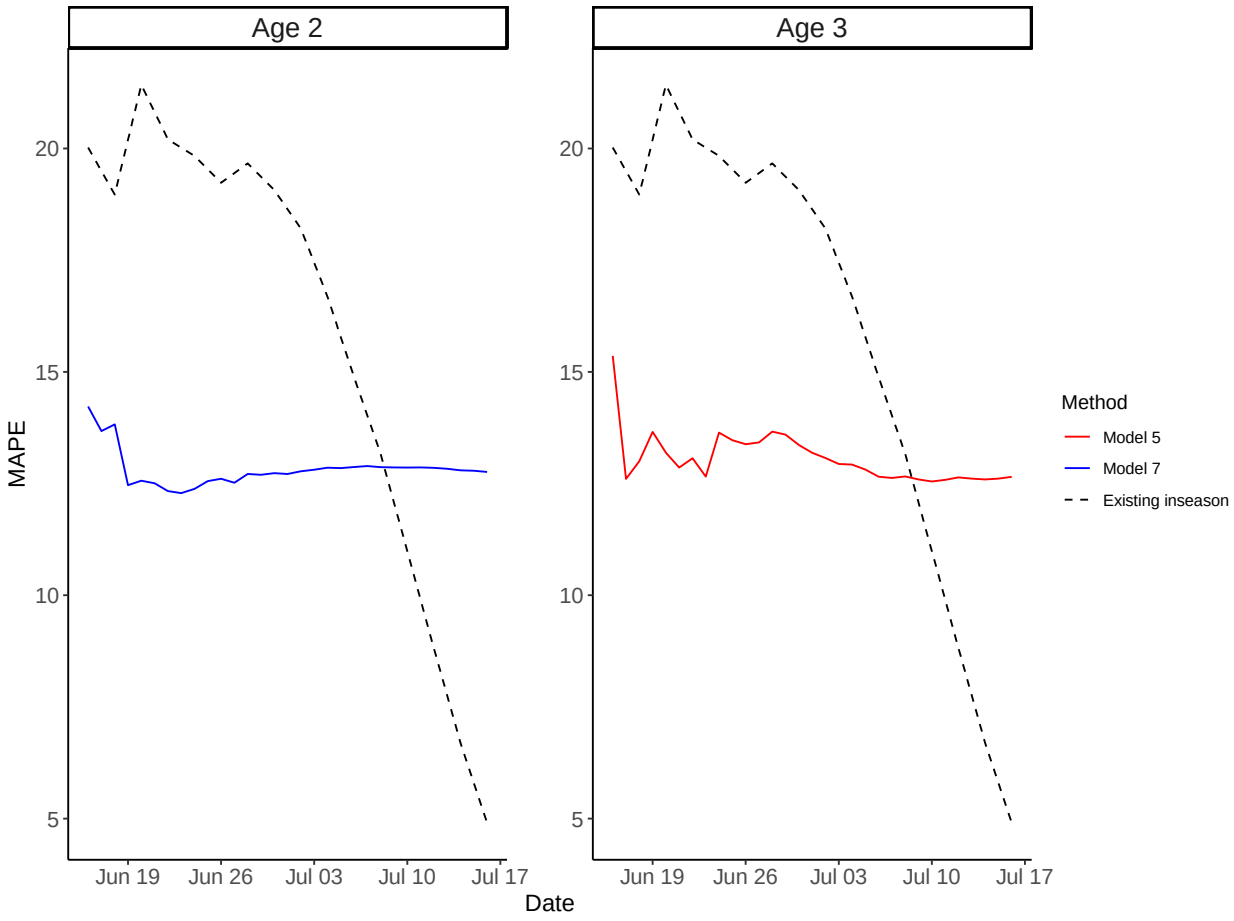

1.8 LITERATURE CITED

Adkison, M.D., and Peterman, R.M. 2000. Predictability of Bristol Bay, Alaska, sockeye salmon returns one to four years in the future. North American Journal of Fisheries Management 20: 69–80.

Dann, T.H., Habicht, C., Baker, T.T., and J.E. Seeb. 2013. Exploiting genetic diversity to balance conservation and harvest of migratory salmon. Canadian Journal of Fisheries and Aquatic Sciences 70: 785–793.

Fried, S.M., and R. Hilborn., 1988. In-Season Forecasting of Bristol Bay, Alaska, Sockeye Salmon (Oncorhynchus-Nerka) Abundance Using Bayesian Probability-Theory. Canadian Journal of Fisheries Aquatic Sciences. 45: 850-855.

Hyun, S.Y., Hilborn, R., Anderson, J.J., and B. Ernst. 2005. A statistical model for in-season forecasts of sockeye salmon (*Oncorhynchus nerka*) returns to the Bristol Bay districts of Alaska. Canadian Journal of Fisheries and Aquatic Sciences 62:1665-1680.

Link, M.R., and R.M. Peterman. 1998. Estimating the value of in-season estimates of abundance

of sockeye salmon (*Oncorhynchus nerka*). Canadian Journal of Fisheries and Aquatic Sciences, 55:1408-1418

Mantua, N.J., Hare, S.R., Zhang, Y., Wallace, J.M., and R.C. Francis. 1997. A Pacific interdecadal climate oscillation with impacts on salmon production. Bulletin of the American Meteorological Society 78: 1069-1080.

Ohlberger, J., Cline, T., Schindler, D.E., and B. Lewis. 2023. Declines in body size of sockeye salmon associated with increased competition in the ocean. Proceedings of the Royal Society 290: 20222248.

Ovando, D., C. Cunningham, P. Kuriyama, C. Boatright, and R. Hilborn. 2022. Improving forecasts of sockeye salmon (*Oncorhynchus nerka*) with parametric and nonparametric models. Canadian Journal of Fisheries and Aquatic Sciences 79: 1198-1210.

Rogers, D.E., and G.T. Ruggerone. 1993. Factors affecting marine growth of Bristol Bay sockeye salmon. Fisheries Research 18: 89-103.

Ruggerone, G.T., and J.R. Irvine. 2018. Numbers and Biomass of Natural- and Hatchery-Origin

Pink Salmon, Chum Salmon, and Sockeye Salmon in the North Pacific Ocean, 1925–2015. Marine and coastal fisheries: Dynamics, management and ecosystem science 10: 152-168.

Ruggerone G.T., Peterman R.M., Dorner B., and K.W. Myers. 2010. Magnitude and trends in abundance of hatchery and wild pink salmon, chum salmon, and sockeye salmon in the north Pacific Ocean. Marine and Coastal Fisheries 2: 306-328.

Staton, B., and M. Catalano. 2019. Bayesian information updating procedures for Pacific salmon run size indicators: evaluation in the presence and absence of auxiliary migration timing information. Canadian Journal of Fisheries and Aquatic Sciences 76: 1719–1727.

Su, Z.M., and M.D. Adkison. 2002. Optimal in-season management of pink salmon (Oncorhynchus gorbuscha) given uncertain run sizes and seasonal changes in economic value. Canadian Journal of Fisheries and Aquatic Sciences: 59:1648-1659.

Tiernan, A., Elison, T., Sands, T., Head, J., Vega, S., and G. Neufeld. 2021. 2020 Bristol Bay Area Annual Management Report. Alaska Department of Fish and Game, Fishery

Management Report No. 21-16, Anchorage.

Tobias, T. M., Waltemyer, D. L., and K.E. Tarbox. 1994. Scale aging manual for upper Cook Inlet sockeye salmon. Regional Information Report No. 2A94-36, Alaska Department of Fish & Game, Anchorage, Alaska.

Ward, E.J., Holmes, E.E., Thorson, J.T., and B. Collen. 2014. Complexity is costly: a meta-analysis of parametric and non-parametric methods for short-term population forecasting. Oikos 123: 652-661.

Chapter 2. RISING TEMPERATURES COULD LEAD TO ZOOPLANKTON POPULATION EXTIRPATION UNLESS MET WITH REDUCTIONS IN SIZE AT MATURITY.

Authors: Grant A. Woodard[1*], Jan Ohlberger[1,2], David Kimmel[3], Max Lindmark[4]

[1]School of Aquatic and Fishery Sciences, University of Washington, Seattle, WA 98195, USA

[2] Washington Department of Fish and Wildlife, 1111 Washington St. SE, Olympia, WA 98501, USA

[3]National Oceanic and Atmospheric Organization, Pacific Marine Environmental Laboratory, 7600 Sand Point Way NE, Seattle, WA 98115

[4]Institute of Marine Research Swedish University of Agricultural Sciences, Department of Aquatic Resources, SLU, Ulls gränd 1, SE-756 51 Uppsala, Sweden

*Correspondence: Email: gwooda@UW.edu

2.1 ABSTRACT

Climate change is warming the earth and its oceans; these trends are expected to continue for the next century. These temperature changes could have major ecosystem impacts starting at the lower trophic levels such as zooplankton and cascading up the system, potentially due to changes in zooplankton size structure with increasing temperatures. Thus, we seek to assess impacts to zooplankton population demographics in the Bering Sea using a physiologically structured population model consisting of a semi chemostat phytoplankton resource and a zooplankton consumer divided into a juvenile and adult stage. Our model predicts that increased temperatures will lead to increased extinction risk starting at around 15 C, but that decreases in size at maturity down to approximately 62 μg would allow the population to persist at higher

temperatures. However, this has the added consequence of a decreased size structure of the population. Such a collapse of the forage base or decrease in size structure could have cascading impacts to the rest of the ecosystem including reductions in carrying capacity and size at age of important fish species.

2.2 INTRODUCTION

Climate change has warmed the Earth on average 0.062 °C each decade between 1900 and 2019 (Garcia-Soto et al. 2021) and scientists project this could increase to as much as 2 °C by the end of the 21st century (IPCC 2014). Changing climate has altered species distributions towards higher elevations and towards the poles, as well as seasonal changes in the timing of life history events (Parmesan & Yohe 2003; Walther 2002). Climate change is also expected to cause a shift towards smaller adult body sizes, particularly for ectotherms (Daufresne et al. 2009; Gardner et al. 2011; Atkinson 1994; Angilletta et al. 2004; but see Audzijonyte et al. 2020). This expectation of smaller adult body sizes at higher temperatures is known as the temperature size rule (TSR) and several mechanisms have been suggested to cause it. First, metabolism increases as a ¾ power of body size (Brown et al. 2004; Gillooly et al. 2001). However, as size increases, an organism's ability to tolerate low oxygen conditions (hypoxia tolerance), though still scaling with size, decreases (Deutsch et al. 2022). This means that larger individuals require a larger reduction in body size to meet reductions in oxygen supply from increased temperature than smaller individuals (Deutsch et al. 2022). Additionally, the TSR may also result from greater

increases in development rates to maturity than growth rates with increasing temperatures, resulting in smaller sizes at age for mature individuals (Berrigan & Charnov 1994; Ohlberger 2013).

The rate of warming for the subarctic North Pacific Ocean is greater than the global average, and by 2050, the Gulf of Alaska is predicted to warm as much as 1.5 °C from 2000 to 2050 (Melillo et al. 2014; Wang et al. 2010), while Bering Sea bottom shelf temperatures may increase by 5 °C by 2100 (Hermann et al. 2019). This could have profound impacts on the species distributions and population structures in the North Pacific Ocean, resulting in large changes to marine ecosystems and valuable commercial fisheries (Dorn et al 2018; Sigler et al. 2011; Grebmeier 2012).

Copepods, many of which have short life histories relative to many vertebrate species (adult female copepods often live for less than a month; Ianora 1998), provide an excellent model organism to assess the population-level implications of increasing temperatures. Though time series copepod data is limited, studies have shown in *Acartia tonsa* and *Acartia hudsonica* in Long Island New York, a decrease in body size from the mid 20th century to 2012 (Rice et al. 2015). Additionally, experiments in mesocosms have demonstrated warmer systems tend to have smaller phytoplankton, zooplankton, and higher turnover of biomass (Garzke et al. 2015; Yvon-Durocher et al. 2015; Yvon-Durocher et al. 2011; Garzke et al. 2016; Peter and Sommer 2012; Peter and Sommer 2013). Copepods also provide a vital link been primary and secondary production in the food chain and provide a food source for all commercial fish species in the

North Pacific Ocean at some life stage (Naganuma, 1996; Kimmel 2011; Wilson et al. 2011; Buckley et al. 2016; Strasburger et al. 2014). Thus, a redistribution towards smaller, more numerous copepods could have impacts on many important commercial fisheries.

Our study seeks to assess changes in the stage structure and population biomass of copepods in the Bering Sea due to ocean temperature increases from climate change, as well as potential implications of changes in size at maturity, using physiologically structured population models (PSPMs). PSPMs link individual level bioenergetics to population size or stage structure using differential equations and allow us to identify equilibrium densities of copepod consumers and resources at various temperatures (de Roos et al. 1992, 2003). This will enable us to explore how *Calanus* (a common genus of copepod in the North Pacific Ocean) populations respond to warmer temperatures and assess the potential impact of any changes in copepod population dynamics and size structure to the ecosystem. We hypothesize that warmer temperatures will cause declining biomass densities and that a smaller size at maturity would allow the population to persist at warmer temperatures than predicted based on current maturation sizes.

2.3 METHODS

2.3.1 MODEL DESCRIPTION

Here we use a PSPM based on that used in Lindmark et al. (2018) with the copepods *Calanus marshallae*/*glacialis,* common in the North Pacific Ocean (Campbell et al. 2016; Nelson et al. 2009) as our model organism to explore the aggregate population level impacts of ocean

warming via effects of changing water temperature on individual physiology. Because *Calanus marshallae/glacialis* are difficult to distinguish morphologically (Choquet et al. 2018; Frost 1974), we will refer to these two species as *Calanus*. *Calanus* start life as an egg, then undergo 6 Nauplii stages, followed by 5 juvenile copepodite stages. These stages are followed by a sixth adult copepodite stage at which somatic growth stops and the copepod allocates all energy towards reproduction.

Our model seeks to make predictions about the densities of the adult (6^{th} copepodite stage) and juvenile (all other) life stages due to changes in temperature. It is composed of two populations, a phytoplankton resource population with semi-chemostat dynamics, and a stage structured *Calanus* consumer population with two stages: a juvenile stage (J) allocating all net production towards somatic growth, and a reproductively mature adult stage (A) that allocates all net production towards reproduction. This model is represented by a system of ordinary differential equations that are dependent on resource density (R), temperature (T), and mass (m) specific rates.

Resource dynamics are dependent on the relationship between phytoplankton resource growth, its carrying capacity in the absence of consumers R_{max}, and ingestion of the phytoplankton resource by the consumer population (equation 1). Here R_{max} represents the maximum phytoplankton density in the absence of consumers, $\delta[T]$ represents the phytoplankton turnover rate (amount of time it takes to replace its biomass), $r_{\delta}(T)$ adds temperature

dependence to the phytoplankton turnover rate, and I_J and I_A represent the ingestion rate by juvenile and adult copepods respectively which follow a Holling type II response (Holling 1959). Equation 5 provides the ingestion rate equation, which is dependent on encounter rate (equation 6), attack rate (equation 7), and maximum ingestion (equation 8). In these formulations, r_I is the temperature dependence of the attack rate (the temperature dependence equation is further described below),

Equation 1 (Phytoplankton): $\frac{dR}{dt} = r_\delta(T)\delta[T](R_{max} - R) - I_J J - I_A A$

The copepod juvenile stage's dynamics (equation 2) are dependent on its accumulation of biomass from growth ($v_J(R,T,m)J$) and adult reproduction ($v_A^+(R,T,m)A$) compared to the juvenile stage's loss of biomass through mortality ($\mu_J(T,m)J$) and maturation ($\gamma\left[v_J^+(R,T,m)\right]J$).

Equation 2 (Juvenile copepods): $\frac{dJ}{dt} = v_A^+(R,T,m)A + v_J(R,T,m)J - \gamma\left[v_J^+(R,T,m)\right]J - \mu_J(T,m)J$

The adult stage's dynamics (equation 3) are dependent on its accumulation of biomass from maturing juveniles entering the adult stage ($\gamma\left[v_J^+(R,T,m)\right]J$) and net production ($v_A(R,T,m)A$) relative to the biomass used for reproduction ($v_A^+(R,T,m)A$) and biomass lost through mortality ($\mu_A(T,m)A$).

Equation 3 (Adult copepods): $\frac{dA}{dt} = \gamma\left[v_J^+(R,T,m)\right]J + v_A(R,T,m)A - v_A^+(R,T,m)A - \mu_A(T,m)A$

We use a general temperature dependence equation (equation 4) from the metabolic theory of ecology (MTE) to make the resource turnover, metabolic, ingestion, and mortality rates temperature dependent. T_0 is the reference temperature at which the parameters were calculated, k is the Boltzmann constant, and E is the activation energy.

Equation 4 (Rate equation based on MTE): $r_Y(T) = e^{E(T-T_0)/kTT_0}$

Ingestion rate (Equation 5) is dependent on an organism's encounter rate and maximum ingestion rate. The encounter rate (equation 6) is in turn dependent on the attack rate $a_{J,A}$ and the resource density R. The attack rate (equation 7) is composed of a temperature dependence component r_I, the maximum attack rate $\hat{A}$, the relationship between the organism's mass $m_{J,A}$ and its optimal mass for feeding m_{opt}, and the allometric exponent α. The maximum ingestion rate (equation 8) in the ingestion rate equation is dependent on a temperature dependence term r_I and the allometric scalar and exponent (ε_1 and ε_2) of the maximum ingestion rate.

Equation 5 (Ingestion rate): $I_{J,A}(R,T,m) = \frac{n_{J,A}(R,T,m)}{1+\frac{n_{J,A}(R,T,m)}{I_{max,J,A}(T,m)}}$

Equation 6 (Encounter rate): $n_{J,A}(R,T,m) = a_{J,A}(T,m)R(T)$

Equation 7 (Attack rate): $a_{J,A}(T,m) = r_I(T)\hat{A}\frac{m_{J,A}}{m_{opt}}e^{(1-m_{J,A}/m_{opt})^{\alpha}}$

Equation 8 (Maximum ingestion rate): $I_{max,J,A}(T,m) = r_I(T)\varepsilon_1 {m_{J,A}}^{\varepsilon_2}$

Net biomass production is calculated as ingestion times assimilation efficiency σ minus metabolism (where ρ_1 and ρ_2 are the allometric scalar and exponent for the metabolic rate and r_M adds temperature dependence). Juveniles mature into adults (equation 11) where z is the size ratio of egg $m_h$to adult m_{mat}. Biomass loss from mortality is incorporated by equation 12 where $\varphi_1$and φ_2 are the allometric scalar and exponent for the mortality rate, and r_μ adds temperature dependence to the mortality rate.

Equation 9 (Metabolic rate): $M_{J,A}(T,m) = r_M(T)\rho_1 {m_{J,A}}^{\rho_2}$

Equation 10 (Net biomass production): $v_{J,A}(R,T,m) = \sigma I_{J,A}(R,T,m) - M_{J,A}(T,m)$

$$v_{J,A}^{+}(R,T,m) = v_{J,A}(R,T,m)\ if\ v_{J,A}(R,T,m) > 0; 0\ otherwise$$

Equation 11 (Maturation rate): $\gamma\left(v_J^{+}(R,T,m)\right) = \frac{v_{J,A}^{+}(R,T,m) - \mu_J(T,m)}{1-z^{1-\frac{\mu_J(T,m)}{v_J^{+}(R,T,m)}}}$

Equation 12 (Mortality rate): $\mu_{J,A}(T,m) = r_\mu(T)\varphi_1 {m_{J,A}}^{\varphi_2}$

2.3.2 MODEL PARAMETERIZATION

Most of the parameters in the model were obtained from the literature for either *Calanus* or other copepods (see Table 2.1). For parameters that were not available from the literature (δ and m_{opt}) either due to lack of information or broad observed ranges, these model parameters were fit to *Calanus* biomass timeseries data. For the resource turnover rate δ, Marañón et al. (2014) identified a range of values occurring in the ocean from under 0.1 to approximately 3.0. We were unable to find a measure of the allometric exponent of attack rate α, but Hjelm and Persson (2001) identified a value of 0.75 in a zooplanktivorous fish which we used as a reference. m_{opt}, the optimal feeding size for *Calanus* on 1 µg phytoplankton was not obtainable from the literature, nor were good estimates given that this parameter can vary widely by species and feeding strategy. Therefore, this parameter was estimated by fitting the model to the observed data but is an area for future experimental studies.

2.3.3 OBSERVATIONAL DATA

To fit the model, mean monthly Bering Sea surface temperature data from the NOAA Physical Sciences Laboratory's NCEP/NCAR Reanalysis monthly means SST dataset was obtained for between 1996 and 2017 (excluding 2013 for which samples were not available) and a mean spring (March through May) and summer (June through August) temperature was calculated for each year. Using these temperatures, we predicted adult and juvenile copepod biomass from the model and compared this to observed mean summer (June through August) Bering Sea *Calanus* biomass densities in these years collected by the Ecosystems and Fisheries

Oceanography Coordinated Investigations (EcoFOCI) program of the Alaska Fisheries Science Center (AFSC). The time series data collected by the EcoFOCI program between 1992 and 2018 were collected during spring and summer months, primarily April and May and August and September. Zooplankton were sampled using oblique tows with paired bongo nets 5-10 m from the bottom while depth was continuously monitored using a SeaBird FastCAT CTD (Incze et al. 1997; Napp et al. 1996; Kimmel and Duffy-Anderson 2020). Bongo nets consisted of one set of 20 cm 153 μm mesh nets and another set of 60 cm 333 or 505 μm mesh nets. Volume of water sampled was estimated with a General Oceanics flowmeter attached to the mouth of the bongo nets. Zooplankton were preserved in a 5% formalin/seawater solution and 150-200 individuals were subsampled with a Folsom plankton splitter and identified to lowest taxonomic level at the Plankton Sorting and Identification Center in Szczecin, Poland and verified at the Alaska Fisheries Science Center, Seattle, Washington, USA. In 2012, a methodological change occurred where the 60 cm frame net mesh was changed to 505 μm. This did not affect most taxa, though there is the potential for differences to arise (Kimmel and Duffy-Anderson 2020). Raw abundance was converted to biomass using literature values for each life-history stage in Gluchowska et al. (2017).

Figure 2.1 shows the *Calanus* density of each sample plotted against the month the sample by EcoFOCI was taken. Adult densities in spring and summer are comparable, though juvenile densities are a bit higher in summer. Additionally, Figure 2.2 shows the number of samples taken each month during this time period, where the vast majority of samples were taken

during May. Thus, the adult and juvenile populations exhibit different characteristics in spring and summer (likely due to life history differences in spring vs summer, since molting into the adult stage and reproduction occurs in late winter/early spring), yet most sampling is in May, followed by September. This means there is a crucial gap in our knowledge of how the population behaves in late spring and summer and because of the clear seasonal differences, fitting models to data from both seasons was difficult. We opted to fit the model to the summer data to ensure that the population persisted at least until the maximum annual mean sea surface temperature was observed. When attempting to fit to spring data, given the similar low densities, the best model fit would predict the population to go extinct at temperatures well below that which it is observed (a problem perpetuated when trying to fit to combined spring and summer data due to the vastly greater amount of spring samples). The two estimated parameters (δ and M_{opt}) were fit by calculating the sum of the square residuals between the observed and predicted biomass densities for each parameter combination and then identifying the parameter combination with the lowest mean sum of squared residuals when averaged across the two life stages. The model was numerically implemented by using the PSPManalysis package in R (de Roos 2021).

One important caveat of the model is that the size at maturity m_{mat} is not temperature dependent (though maturation rate is). Therefore, to assess if smaller sizes at maturity would allow population persistence as temperatures warm, an indicator of the evolutionary trend the population might take, we also ran the model using the above fit parameters while varying the

size at maturity to assess if this would impact the population's ability to persist at warmer temperatures. This application of the model also allowed us to assess if changes in size at maturity would be associated with changes in the adult to juvenile biomass density ratio, an indicator of the population's stage and size structure.

2.4 RESULTS

Observed mean summer *Calanus* densities were highly variable over the study period, ranging from near 0 to over 80 µg/L (figure 2.3). Adult biomass densities were comparable in spring and summer, whereas juvenile biomass densities were much greater in summer. On average, mean spring and summer sea surface temperatures increased slightly from 1996 to 2017 though there was a cold period from 2006 to 2012 (figure 2.4). Spring sea surface temperatures ranged between approximately -3.3 and 2.1 °C. Summer sea surface temperatures ranged between approximately 5.6 and 9.8 °C.

Our model generated per capita and aggregate population metrics of physiological rates consistent with our application of the MTE (figure 2.5). Per capita rates follow an exponential increase with temperature, whereas aggregate population rates are hump shaped except for the resource turnover rate (H). This is because while the model predicted decreases in adult and juvenile *Calanus* biomass densities with increasing temperature (figure 2.6), the phytoplankton resource biomass density increased with increasing temperature as the total amount of ingestion exerted by the consumer population decreased. Thus, for the *Calanus* aggregate population rates,

low population abundances combined with high per capita ingestion, metabolism, and mortality rates at high temperatures combined to produce the hump shaped curves, whereas for the phytoplankton turnover, increasing biomass densities combined with an increasing per capita turnover rate resulted in an exponential relationship between aggregate phytoplankton turnover and temperature.

Our model was able to predict *Calanus* biomass densities on the order of those observed in the field (figure 2.7). Model fit minimized the average sum of squared residuals between observed and predicted biomass densities among years with a resource turnover rate δ of 0.01 day^{-1} and optimal forager size m_{opt} of 96 µg. Our model predicts net production to be maximized with a value of 10.19 µg/day at 5.6 °C (figure 2.8), well below the observed mean maximum summer temperature between 1992 and 2018 of 9.8 °C. The population birth rate was maximized at 0.64 at a slightly higher temperature of 7.07 °C. Population extirpation occurred at temperatures slightly below 15 °C under the above model parameters. However, decreasing the size at maturity m_{mat}, resulted in an increase in the biomass density at this temperature and allowed the population to persist at even warmer temperatures (figure 2.9, figure 2.10 A), indicating that decreases in size at maturity down to some threshold may allow the population to persist at higher temperatures. When varying the size at maturity at the lowest extinction temperature (14.8 °C) to assess how changes in size at maturity might affect a persisting population's size structure, the adult to juvenile biomass density ratio decreased as size at maturity increased (figure 2.10 B), reaching a ratio of 0.15 at a size at maturity of 265 µg. The

adult to juvenile biomass density ratio at the size at maturity threshold (62 μg) where further decreases in the size at maturity did not result in additional biomass increases was 0.24. Thus, from the initial size at maturity of 265 μg to the size at maturity threshold, the adult to juvenile ratio increased by 0.09.

2.5 DISCUSSION

Our model predicts biomass densities similar to those observed in the field. The model further predicts that given our set of parameters, population biomass reaches zero as temperatures approach 15 °C. This temperature is substantially below the lethal temperatures for closely related *Calanus finmarchicus* observed in the laboratory which range between 24 and 26 °C (Marshall 1935). This means that average summer sea surface temperatures which currently reach 9.8 °C are already above those that maximize net production and birth rate of *Calanus* and nearing temperatures at which we would expect a rapid decline in population biomass and associated increase in phytoplankton biomass as total consumer ingestion decreases.

This decline in zooplankton biomass and increase in phytoplankton biomass with increasing temperature is generally consistent with findings in many ecosystem models, though there is high variability among predictions (Megrey et al. 2007; Morán et al. 2009; Woodworth-Jefcoats et al. 2017). Declines in zooplankton biomass would substantially reduce an important food source in the North Pacific Ocean, with potential cascading impacts to forage fish, commercial fish species, and cetaceans and sea birds. Recent ecosystem-based models predict decreases in zooplankton biomass associated with climate change will lead to reductions in

carrying capacity for commercially important pelagic fish species by as much as 20-50% (Woodworth-Jefcoats et al. 2017). Megrey et al. (2007) predicted decreases in zooplankton biomass and slower growth and smaller weights at age in two species of forage fish.

Our model predicts that the aforementioned extirpation, as summer temperatures approach 15 °C, may be avoided with decreases in size at maturity, though this will likely have consequences for the ratio of adult to juvenile biomass densities and the size distribution of the population. In particular, our model predicts slight increases in the adult to juvenile biomass density ratio as size at maturity decreases at a given temperature. Shifts in zooplankton size structure are not expected to substantially impact ecosystem biomass alone, but when combined with other climate issues like changes in phytoplankton populations, decreases in dissolved oxygen, and ocean acidification, may decrease ecosystem biomass by 30% (Ainsworth et al. 2011).

One important caveat is our use of sea surface temperatures in the model because they are readily available. The Bering Sea is a stratified system and is warmer at the surface than at the bottom. Copepods use diel vertical migration, feeding near the surface at night and returning to deeper water for the day. This serves to minimize predation risk during feeding but also has the benefit of reducing the duration of exposure to warmer temperatures at the surface. Thus, because deep water and nighttime foraging near the surface provide thermal refuges for copepods during a large portion of their lives, they likely would be able to persist at sea surface

temperatures above 15 °C. Therefore, our model's prediction of this temperature threshold can be considered the minimum temperature at which extirpation would be a concern.

Another important note is that the pattern of shifts in population sizes and community sizes depends not only on within species shifts in size or stage ratios, but also on compositional shifts in the species present (Martins et al. 2023). Thus, community size composition could also change via the addition or removal of species, and this in turn could impact size distributions within a population in the same or opposite direction as within species changes in population size. It is the combination of these intraspecific and compositional effects that determine the overall direction of size trends both within a population and community (Martins et al. 2023). Our model only has one species of consumer and thus cannot account for the effects changes in species composition may have on *Calanus* size structure.

Despite these limitations, our simple PSPM successfully predicts *Calanus* densities on the orders of those observed in the North Bering Sea and emulates many of the predicted climate effects to zooplankton populations such as decreasing biomass with increasing temperature. It additionally predicts that smaller sizes at maturity would allow the population to persist at higher temperatures. The prediction that population densities approach zero at approximately 15 °C if the population is unable to adapt is concerning given that temperatures are predicted to approach this threshold by 2100 (Hermann et al. 2019). This extirpation can be avoided with decreases in size at maturity, but only if the population's adaptive capacity outpaces ocean warming. Declines in biomass and size at maturity would have potential negative and cascading impacts to forage

and commercial fish species. Future research would benefit from more data collection during the periods of greatest temperature change (June) and more consistent sampling across seasons to develop a model that can better incorporate these seasonal differences in temperature and biomass. We also intend to develop the model in the future to have a higher mortality rate to better mimic natural systems with many zooplanktivores.

2.6 TABLES

Table 2.1. Parameter values from the literature and estimates.

Symbol	Value	Unit	Interpretation	Reference
Resource Dynamics				
$\boldsymbol{\delta}$	**0.01**	day^{-1}	Resource turnover rate	Estimated from model fit to observed data. Range of between approximately .1 and 3 from Marañón et al. (2014)
R_{max}	2000	µg C/L	Maximum resource density in the absence of consumers	Approximated from Putland and Iverson (2007
E_{δ}	0.5	eV	Activation energy of resource turnover rate	(Barton and Yvon-Durocher 2019)
Consumer Dynamics				
m_{mat}	265.07	µg	Size at maturity	(Petersen 1986)
m_h	0.75	µg	Egg mass	(Petersen 1986)

$\hat{A}$	0.096	L/day	Maximum attack rate	(Frost 1972)
α	0.75	-	Allometric exponent of attack rate	Approximately 0.75 for fish (Hjelm and Persson 2001)
ε_1	2.30	$\mu g^{(1-\varepsilon_2)} day^{-1}$	Allometric scalar of maximum ingestion rate	(Saiz and Calbet 2007)*
ε_2	0.70	-	Allometric scalar of maximum ingestion rate	(Saiz, and Calbet 2007)*
E_I	0.46	eV	Activation energy of ingestion rate	(Maps et al. 2012)
ρ_1	11.59	$\mu g^{(1-\rho_2)} day^{-1}$	Allometric scalar of metabolic rate	Ikeda et al. 2007**
ρ_2	0.75		Allometric exponent of metabolic rate	Ikeda et al. 2007**
E_M	.55	eV	Activation Energy of Metabolism	(Maps et al. 2014)
z		-	Egg to adult size ratio	(Petersen, 1986)
φ_1	1.336596	$\mu g^{(1-\varphi_2)} day^{-1}$	Allometric scalar of mortality rate	(Hirst and Kiørboe 2002)
φ_2	-0.092	-	Allometric exponent of mortality rate	(Hirst and Kiørboe 2002)
E_μ	.57	eV	Activation energy of background mortality	(McCoy and Gillooly 2008)

$\underline{\sigma}$	0.7	-	Assimilation efficiency	(de Roos et al. 2007; Peters 1983; Yodzis and Innes 1992)
$\boldsymbol{m_{opt}}$	**96**	µg	Optimal forager size for 1 µg algae	Estimated from model fit to observed data
Environmental Parameters				
k	8.617e-5		Boltzmann constant	
T	Varied	K	Temperature	
$T_{0,\delta}$	281.15	K	Reference temperature of turnover rate	Reference temperature for a turnover rate of 1 from Marañón et al. (2014).
$T_{0,\varepsilon}$	288.15	K	Reference temperature of ingestion allometric scalar and exponent	(Saiz, and Calbet 2007)
$T_{0,\rho}$	275.15	K	Reference temperature of metabolism allometric scalar and exponent	Ikeda et al. 2007
$T_{0,\varphi}$	288.15	K	Reference temperature of background mortality allometric scalar and exponent	(Hirst and Kiørboe 2002)

*Estimated using linear regression from Saiz, and Calbet (2007) maximum ingestion data (log transformed) and mass data for copepods at 15 °C.

**Obtained by fitting a linear regression model to respiration data (log transformed) and mass data taken at 2 °C from Ikeda et al. 2007.

2.7 FIGURES

Figure 2.1. Month and density of each Calanus sample from 1996 to 2017 (excluding 2013).

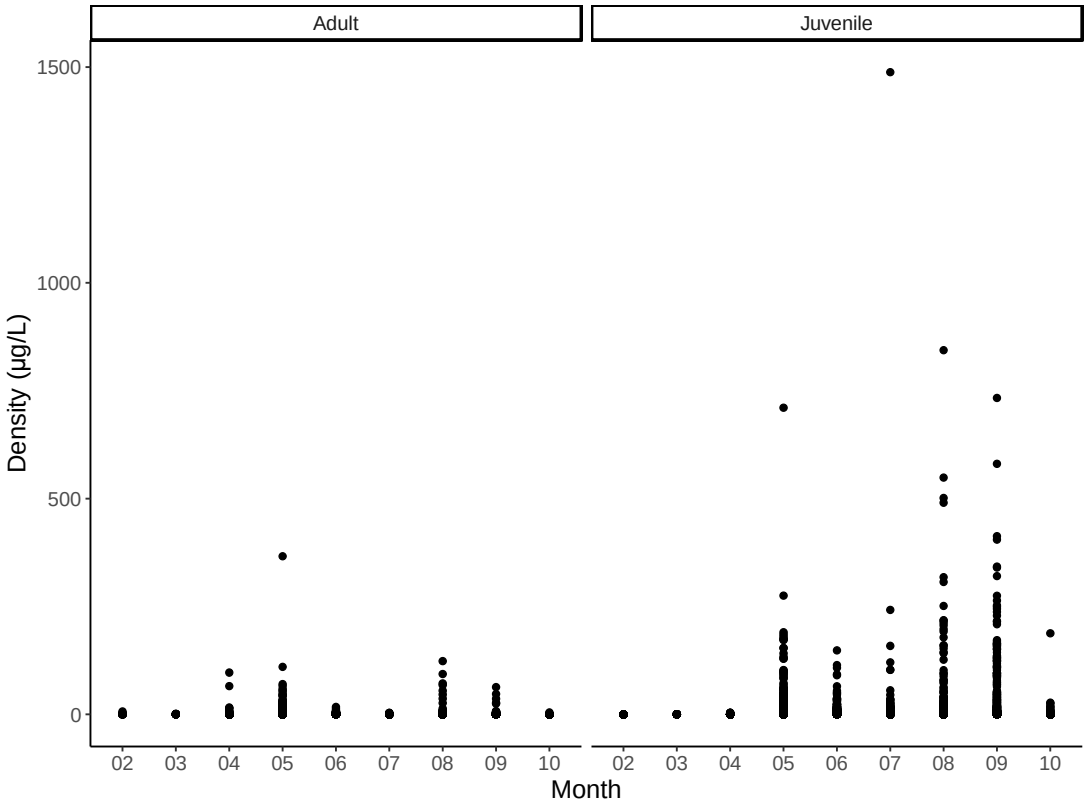

Figure 2.2. The number of samples taken each month from 1992 to 2018.

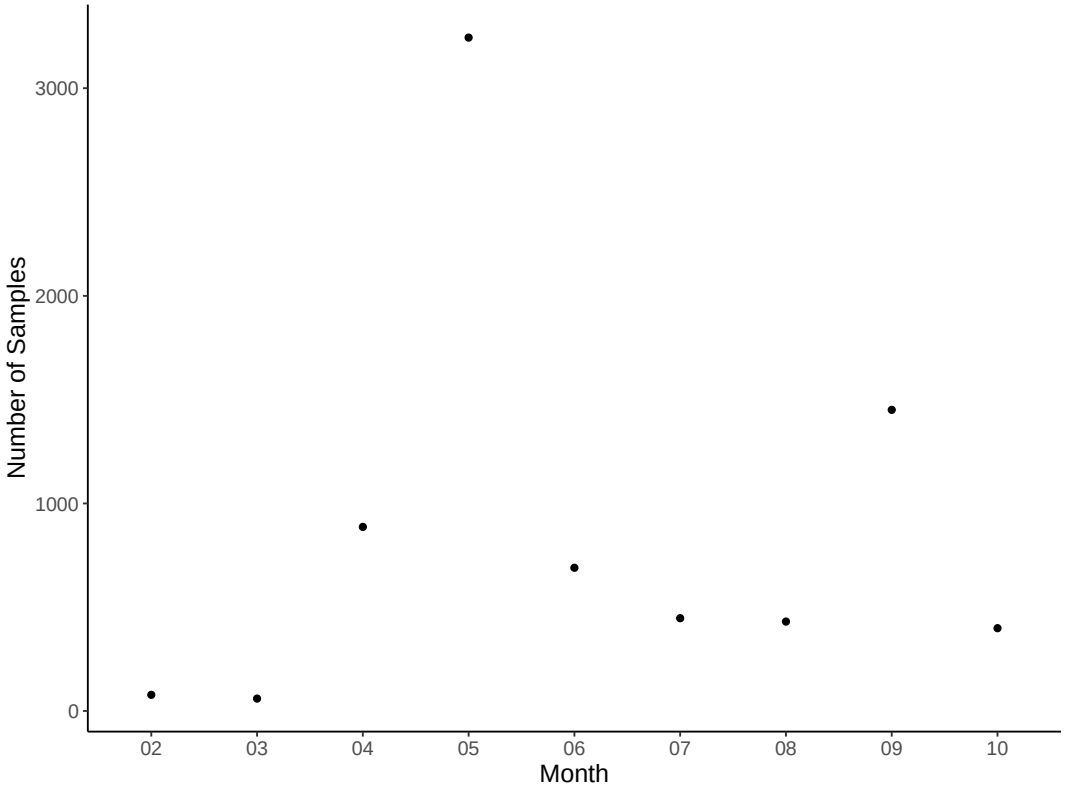

Figure 2.3. Observed *Calanus marshallae* biomass densities in the Bering Sea between 1996 and 2017 (excluding 2013).

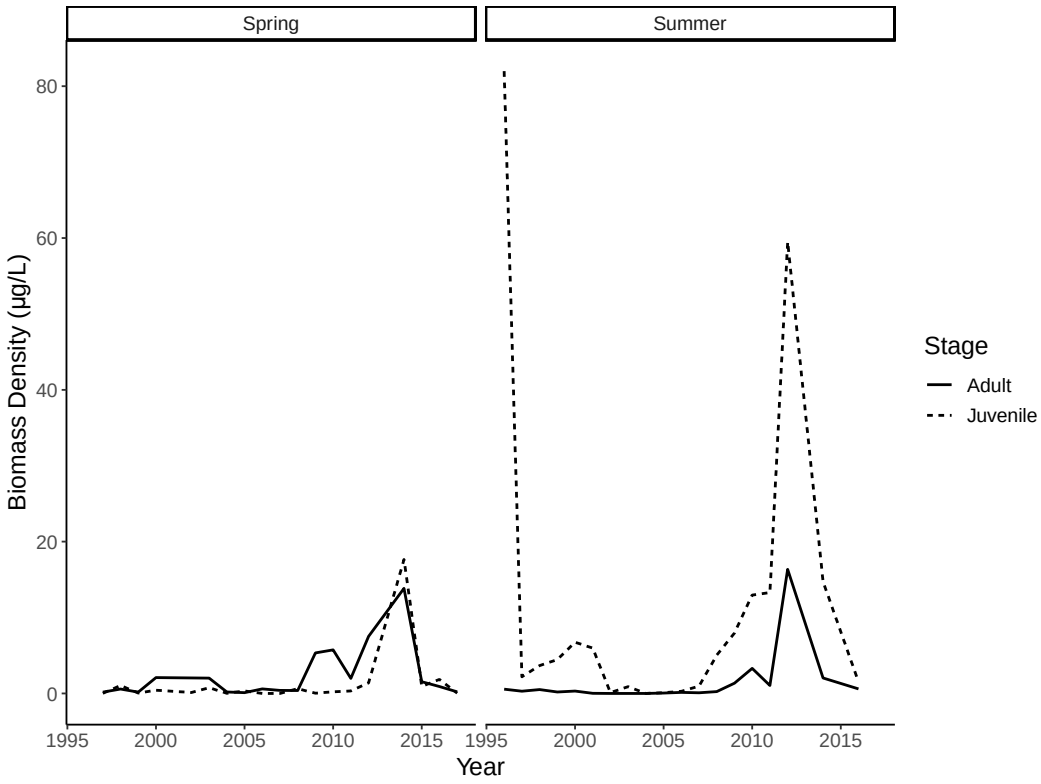

Figure 2.4. Observed mean sea surface temperatures in spring and summer for the Bering Sea.

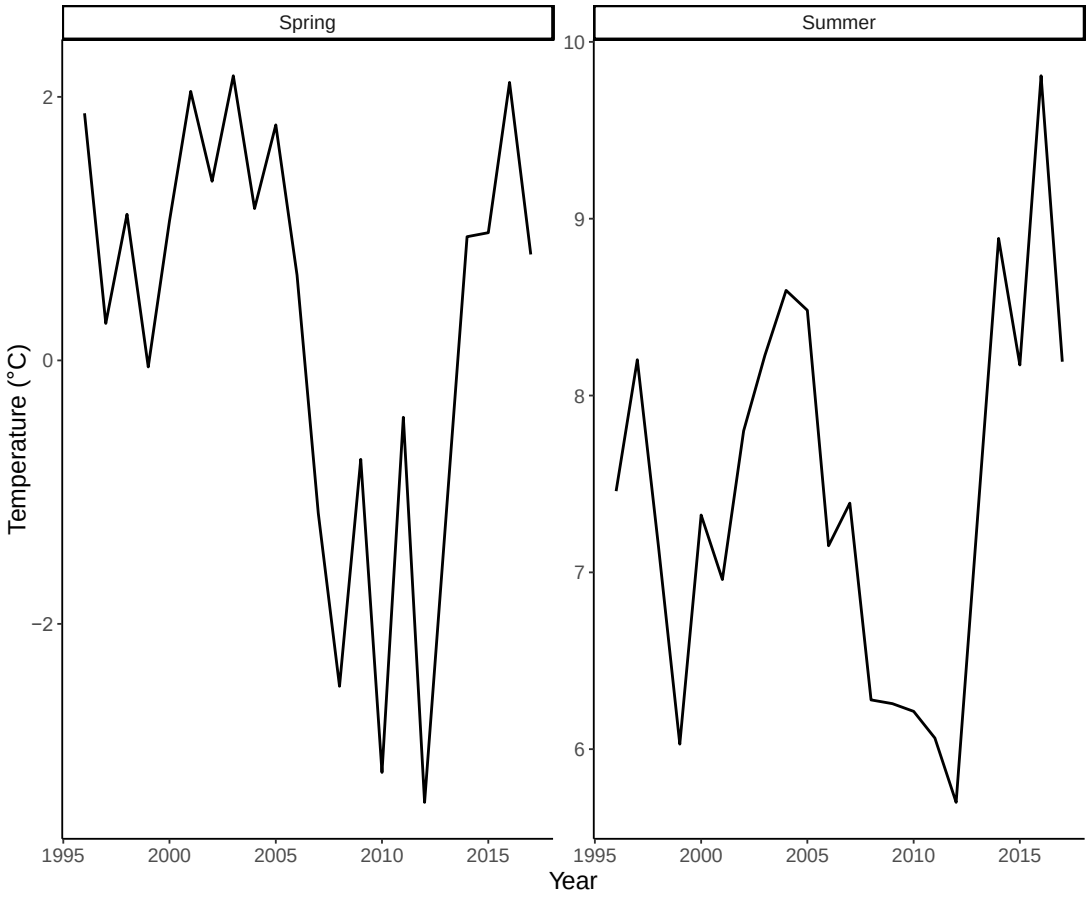

Figure 2.5. Physiological rates on a per capita (A through D) and population (E through H) basis predicted in the model.

For the ingestion plots, the dotted line represents the maximum ingestion rate, while the solid line represents the applied ingestion rate.

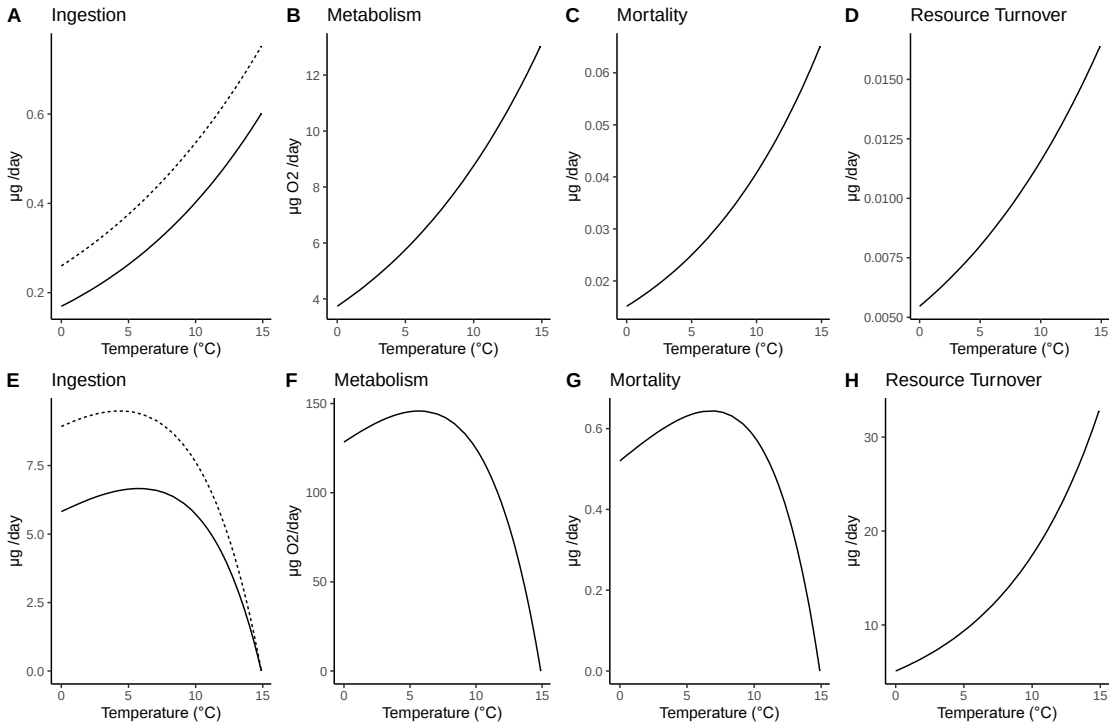

Figure 2.6. Population trajectories predicted by the model with changes in temperature.

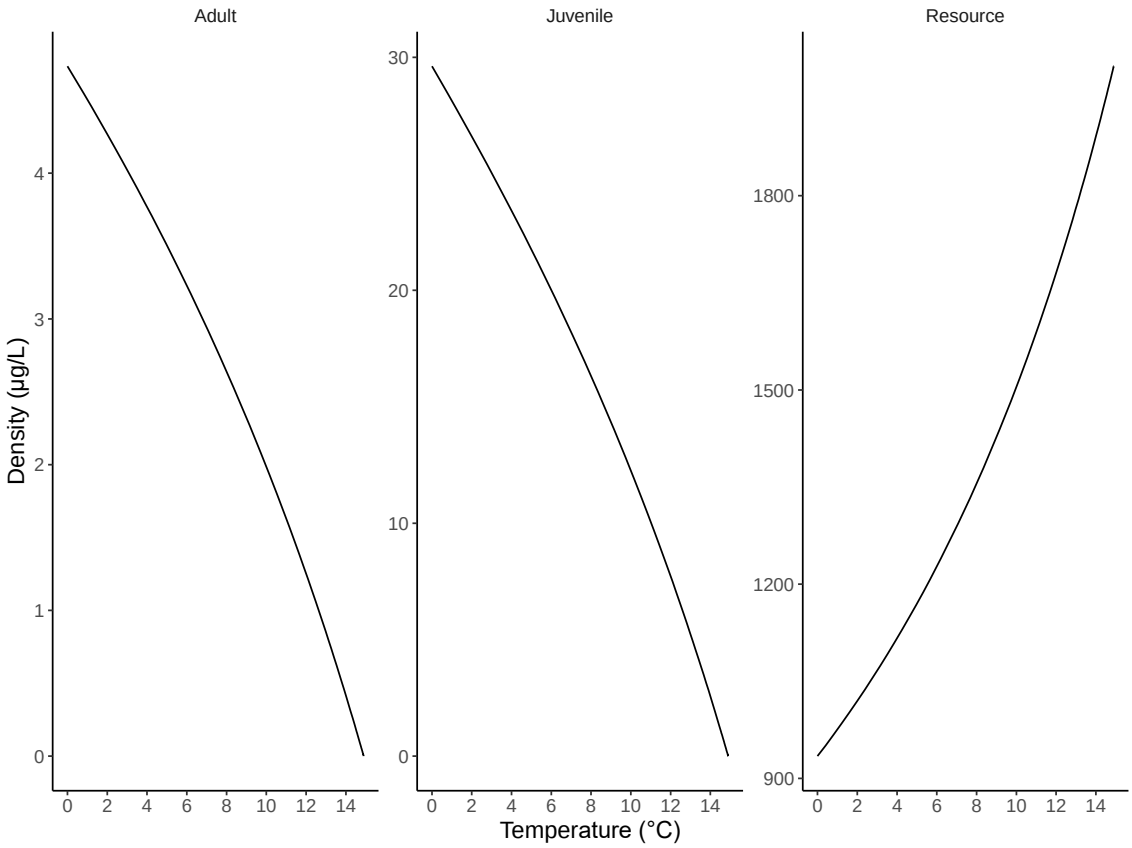

Figure 2.7. Observed vs predicted *Calanus* biomass densities at observed mean summer sea surface temperatures from 1996 to 2017 (excluding 2013).

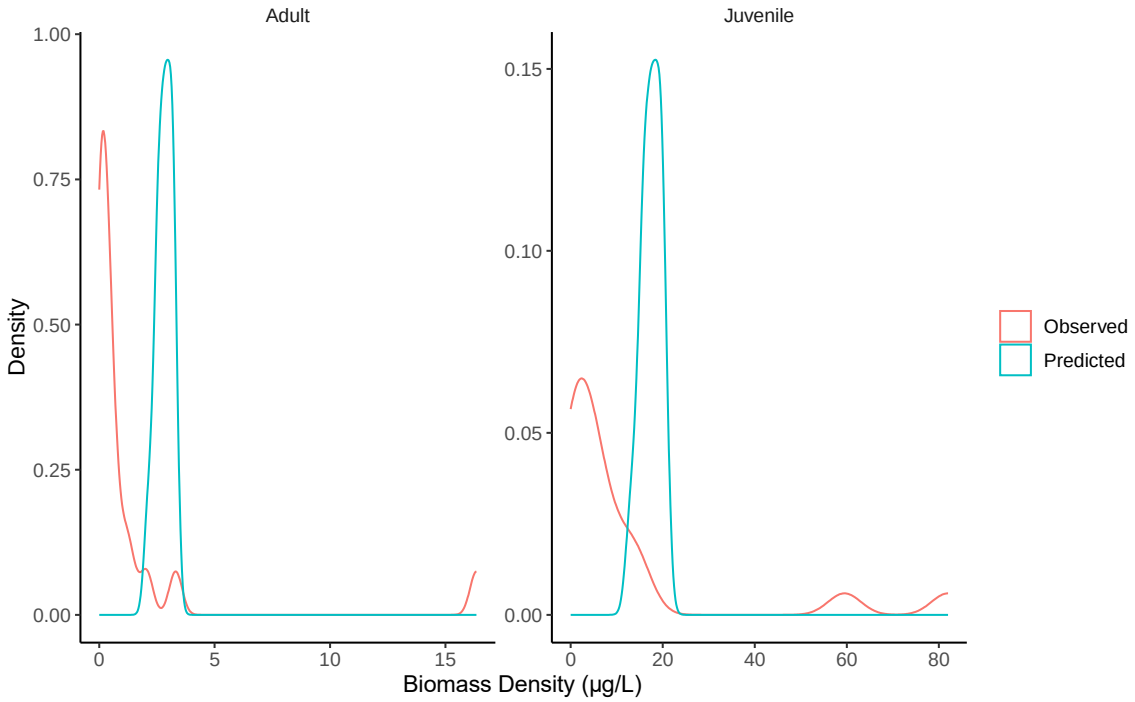

Figure 2.8. Predicted per capita and population level birth rate and net production with changes in temperature.

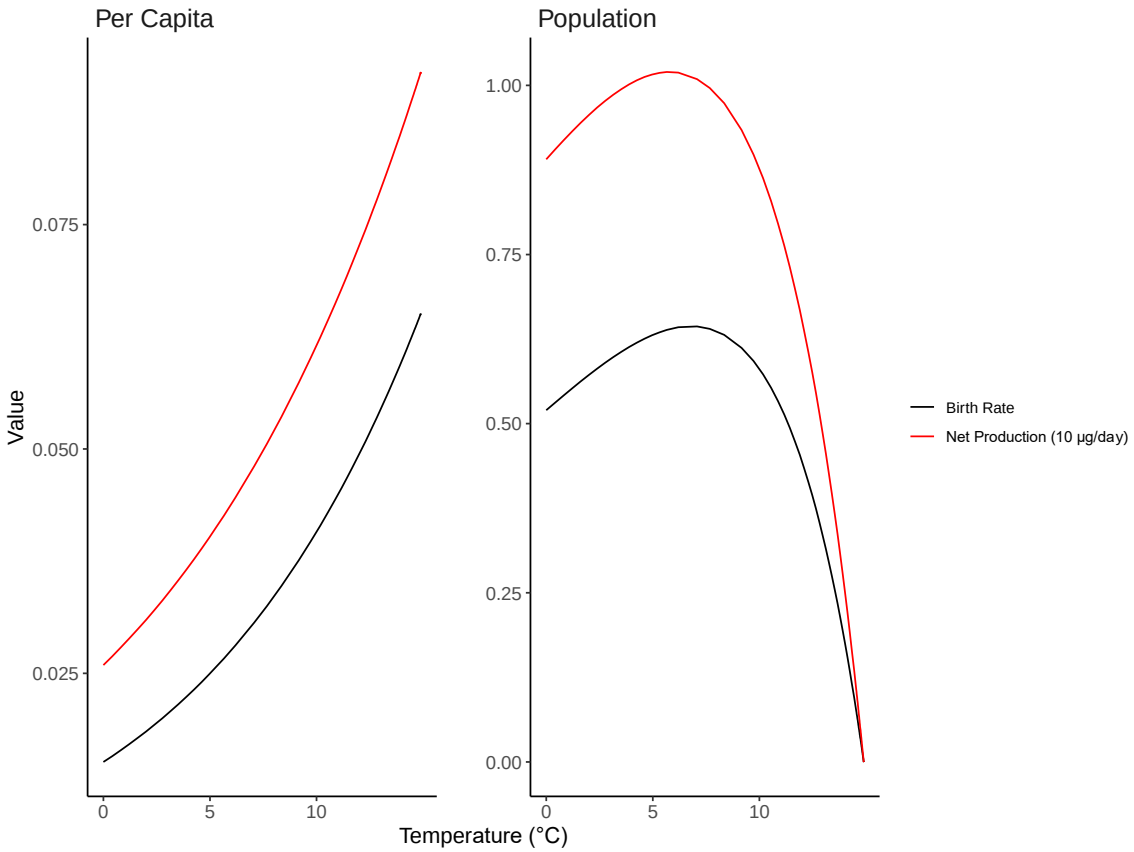

Figure 2.9. Extinction temperature vs size at maturity.

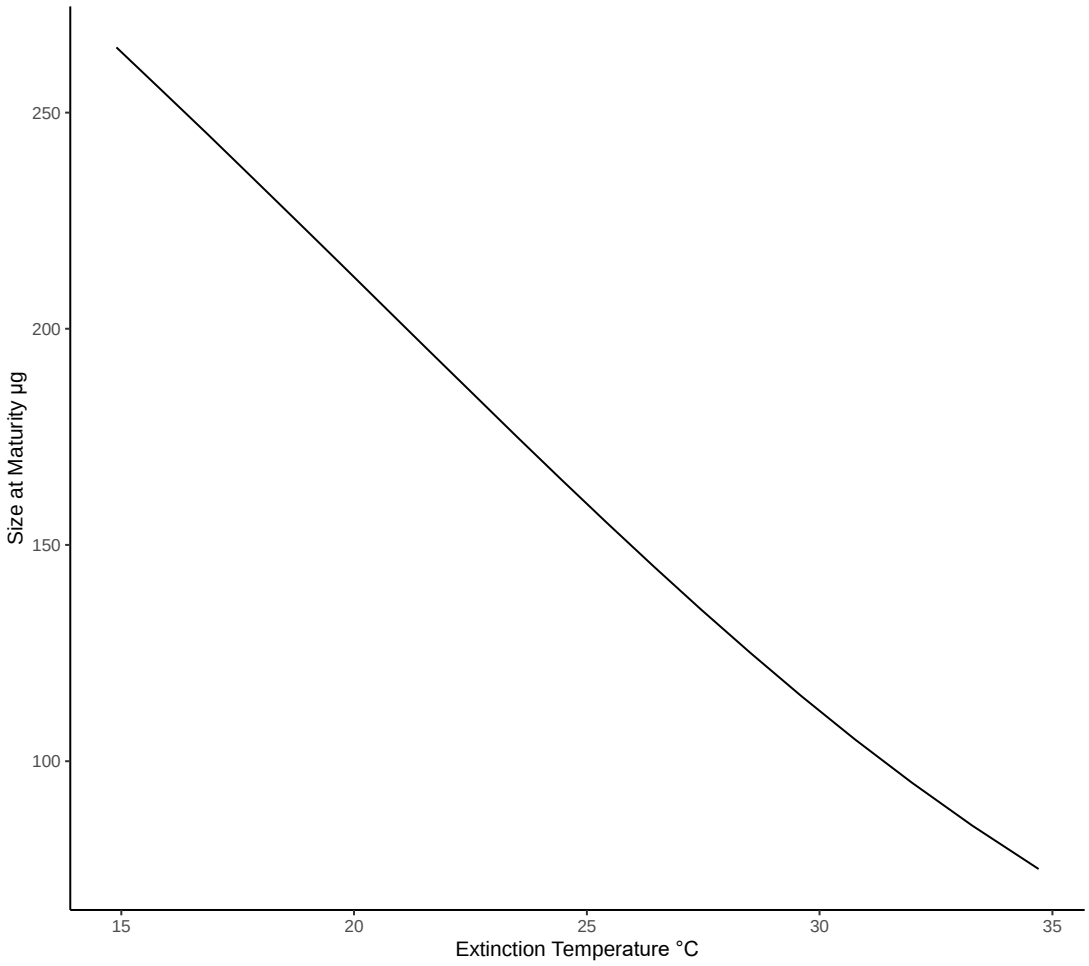

Figure 2.10. Size at maturity vs biomass density at 14.8 °C (A) and the change in the adult to juvenile biomass density ratio with changes in size at maturity at this temperature (B).

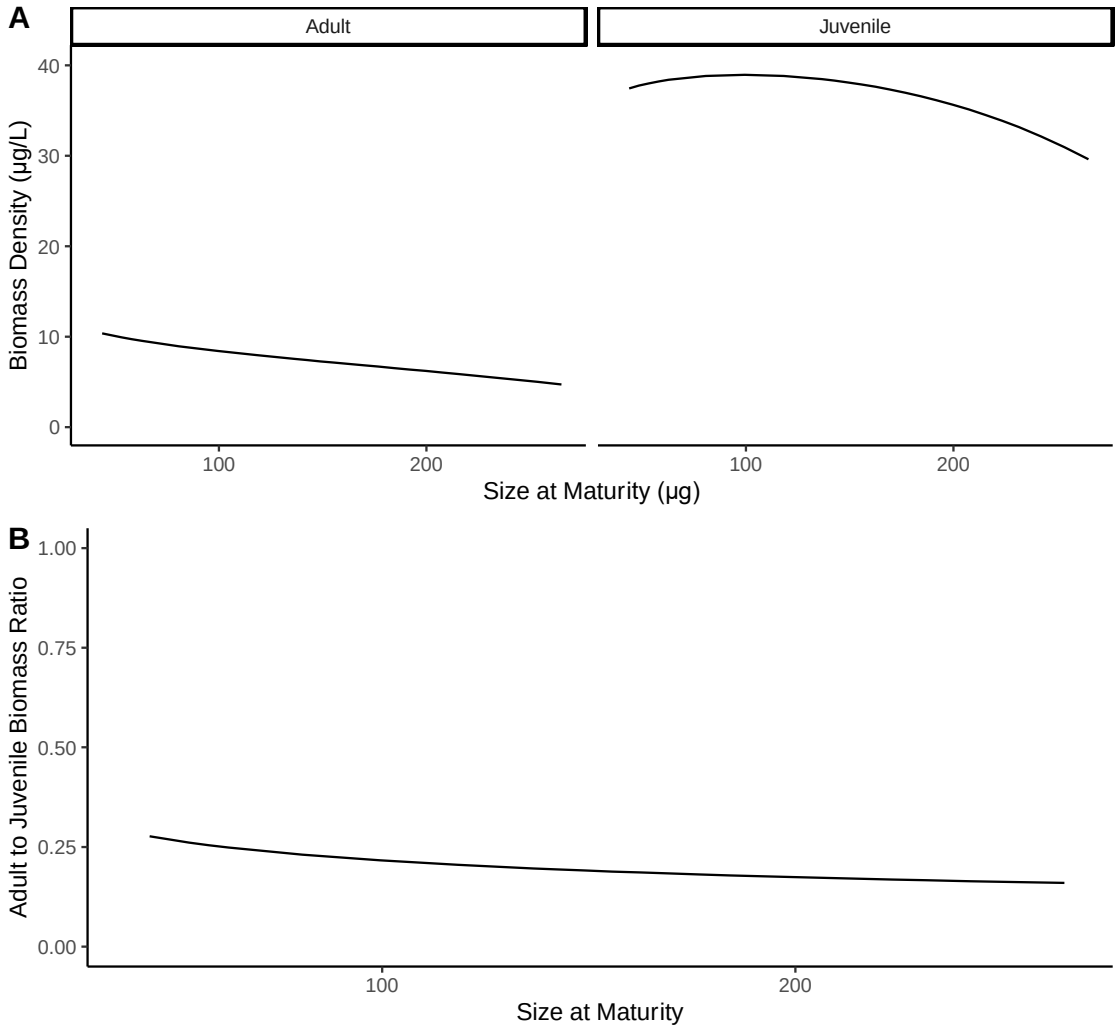

2.8 LITERATURE CITED

Ainsworth, C.H., Samhouri, J.F., Busch, D.S., Cheung, W.W.L. Dunne, J., and T.A. Okey. 2011. Potential impacts of climate change on Northeast Pacific marine foodwebs and fisheries. ICES Journal of Marine Science, 68: 1217-1229.

Atkinson, D. 1994. Temperature and organism size - a biological law for ectotherms? Advances in Ecological Research 25: 1-58.

Angilletta, M. J., Steury, T. D. & M.W. Sears. 2004. Temperature, growth rate, and body size in ectotherms: fitting pieces of a life-history puzzle. Integrative and Comparative Biology. 44: 498-509.

Audzijonyte, A., Richards, S. A., Stuart-Smith, R. D., Pecl, G., Edgar, G. J., Barrett, N. S., Payne, N., & Blanchard, J. L. 2020. Fish body sizes change with temperature but not all species shrink with warming. Nature Ecology & Evolution 4, 809–814.

Barton, S. and Yvon-Durocher, G. 2019, Quantifying the temperature dependence of growth rate in marine phytoplankton within and across species. Limnology and Oceanography 64:

2081-2091.

Berrigan, D. & Charnov, E. 1994. Reaction norms for age and size at maturity in response to temperature: a puzzle for life historians. *Oikos*, **70**, 474–478.

Brown, J. H., Gillooly, J. F., Allen, A. P., Savage, V. M. & G.B. West. 2004. Toward a metabolic theory of ecology. Ecology 85: 1771-1789.

Buckley, T. W., Ortiz, I., Kotwicki, S. & K. Aydin. 2016. Summer diet composition of walleye pollock and predator–prey relationships with copepods and euphausiids in the eastern Bering Sea, 1987–2011. Deep Sea Research Part II: Topical Studies in Oceanography 134: 302-311.

Campbell, R.G. et al. 2016. Mesozooplankton grazing during spring sea-ice conditions in the eastern Bering Sea. Deep-Sea Research Part II: Topical Studies in Oceanography 134: 157-172.

Choquet M, Kosobokova K, Kwasniewski S, Hatlebakk M, Dhanasiri A.K.S, Melle W, Daase M, Svensen C, Soreide JE., and G. Hoarau. 2018. Can morphology reliably distinguish

between the copepods Calanus finmarchicus and C glacialis, or is DNA the only way? Limnology and Oceanography-Methods 16:237-252

Daufresne, M., Lengfellner, K. & U. Sommer. 2009. Global warming benefits the small in aquatic ecosystems. Proceedings of the National Academy of Science USA 106:12788-12793.

de Roos, A.M., Schellekens, T. van Kooten, T., van de Wolfshaar, K., Claessen, D. and L. Persson. 2007. Food-dependent growth leads to overcompensation in stage-specific biomass when mortality increases: The influence of maturation versus reproduction regulation. The American Naturalist, 170: E59-E76.

de Roos, A.M. et al. 2008. Simplifying a physiologically structured population model to a stage-structured biomass model. Theoretical Population Biology 73: 47-62.

de Roos, A. M., Diekmann, O. & J.A.J., Metz. 1992. Studying the dynamics of structured population models - a versatile technique and its application to *Daphnia*. American Naturalist 139: 123-147.

de Roos, A.M., 2021. PSPManalysis. A package for numerical analysis of physiologically structured population models. https://CRAN.R-project.org/package=PSPManalysis.

Dorn, M. et al. 2018. A climate science regional action plan for the Gulf of Alaska. US Department of Commerce, National Oceanic and Atmospheric Administration.

Deutsch, C. Penn, J.L. W.C.E.P., Verbek, and J.L. Payne. 2022. Impact of warming on aquatic body sizes explained by metabolic scaling from microbes to macrofauna. Proceedings of the National Academy of Sciences 119: 1-9.

Frost, B.W. 1972. Effects of size and concentration of food particles on the feeding behavior of the marine planktonic copepod *Calanus pacificus*. Limnology and Oceanography 17: 805-815.

Frost, B.W. 1974. *Calanus marshallae*, a new species of calanoid copepod closely allied to the sibling species *C. finmarchicus* and *C. glacialis*. Marine Biology 26: 77-99.

Garcia-Soto C., Cheng L., Caesar L., Schmidtko S., Jewett E.B., Cheripka A., Rigor I., Caballero A., Chiba S, Báez J.C., Zielinski T. and J.P. Abraham. 2021. An overview of ocean

climate change indicators: Sea surface temperature, ocean heat content, ocean pH, dissolved oxygen concentration, arctic sea ice extent, thickness and volume, sea level and strength of the AMOC (Atlantic Meridional Overturning Circulation). Frontiers in Marine Science 8:642372.

Gardner, J. L., Peters, A., Kearney, M. R., Joseph, L. & R. Heinsohn. 2011. Declining body size: a third universal response to warming? Trends in Ecology & Evolution 26: 285-291.

Garzke, J., Ismar, S. M. H. & U. Sommer. 2015. Climate change affects low trophic level marine consumers: warming decreases copepod size and abundance. Oecologia 177: 849-860.

Garzke, J., Hansen, T., Ismar, S. M. H. & U. Sommer. 2016. Combined Effects of Ocean Warming and Acidification on Copepod Abundance, Body Size and Fatty Acid Content. PLoS One 11.

Gillooly, J. F., Brown, J. H., West, G. B., Savage, V. M. & E.L. Charnov. 2001. Effects of size and temperature on metabolic rate. Science 293: 2248-2251.

Gluchowska, M., Dalpadado, P., Beszczynska-Moller, A., Olszewska, A., Ingvaldsen, R.B., and

S. Kwasniewski. 2017. Interannual zooplankton variability in the main pathways of the Atlantic water flow into the Arctic Ocean (Fram Strait and Barents Sea branches). ICES Journal of Marine Science, 74: 1921−1936.

Grebmeier, J.M. 2012. Shifting patterns of life in the Pacific Arctic and sub-Arctic seas. Annual Review of Marine Science 4: 63-78.

Hermann AJ, Gibson GA, Cheng W, Ortiz I, Aydin K, Wang M, Hollowed AB, Holsman KK, and S. Sathyendranath. 2019. Projected biophysical conditions of the Bering Sea to 2100 under multiple emission scenarios. ICES Journal of Marine Science 76:1280-1304.

Hjelm, J. & Persson, L. 2001. Size-dependent attack rate and handling capacity: inter-cohort competition in a zooplanktivorous fish. *Oikos,* 95**,** 520-532.

Hunt, G. L., Jr. et al. 2011. Climate impacts on eastern Bering Sea foodwebs: a synthesis of new data and an assessment of the Oscillating Control Hypothesis. ICES Journal of Marine Science 68: 1230-1243.

Huntley, M.E. and M.D.G. Lopez. 1992, Temperature-Dependent Production of Marine

Copepods: A Global Synthesis. The American Naturalist 140: 201-242.

Holling, C. S. 1959. The components of predation as revealed by a study of small mammal predation of the European pine sawfly. Canadian Entomology 91: 93–320.

Ianora, A. 1998. Copepod life history traits in subtemperate regions. Journal of Marine Systems, 15: 337-349.

Incze, L. S., Siefert, D. W. & J.M. Napp. 1997. Mesozooplankton of Shelikof Strait, Alaska: Abundance and community composition. Continental Shelf Research 17: 287-305.

Ikeda, T., Sano, F., and Yamaguchi, A., 2007. Respiration in marine pelagic copepods: a global-bathymetric model. Marine Ecology Progress Series 339: 215-219

Intergovernmental Panel on Climate Change (IPCC). 2014. Climate Change 2014: Synthesis Report. Contribution of Working Groups I, II and III to the Fifth Assessment Report of the Intergovernmental Panel on Climate Change.

Kimmel, D. G. 2011. Trophic Relationships of Coastal and Estuarine Ecosystems. Treatise on Estuarine and Coastal Science. eds Wilson J.G., & Luczkovich, J.J., Academic Press.

Kimmel D.G., and J.T. Duffy-Anderson. 2020. Zooplankton abundance trends and patterns in Shelikof Strait, western Gulf of Alaska, USA, 1990–2017. Journal of Plankton Research 42:334-354.

Lindmark, M., Huss, M., Ohlberger, J. & A. Gårdmark. 2018. Temperature-dependent body size effects determine population responses to climate warming. Ecology Letters 21, 181-189.

Marshall S.M., Nicholls A.G., and A.P. Orr. 1935. On the biology of *Calanus finmarchicus*. Part VI. Oxygen consumption in relation to environmental conditions. Journal of the Marine Biological Association of the United Kingdom. 20: 1-27.

Martins, I.S. et al. 2023. Widespread shifts in body size within populations and assemblages. Science, 381: 1067-1071.Maps, F., Pershing, A.J., and N.R. Record. 2012. A generalized approach for simulating growth and development in diverse marine copepod species. ICES Journal of Marine Science 69: 370-379.

Maps, F., Record, N.R., and A. Pershing. 2014. A metabolic approach to dormancy in pelagic

copepods helps explaining inter- and intra-specific variability in life-history strategies. Journal of Plankton Research 36: 18-30.

Marañón E, Cermeño P, Huete-Ortega M, López-Sandoval DC, Mouriño-Carballido B, et al. 2014. Resource Supply Overrides Temperature as a Controlling Factor of Marine Phytoplankton Growth. PLOS ONE 9: e99312

McCoy, M.W., and J.F. Gillooly. 2008. Predicting natural mortality rates of plants and animals. Ecology Letters 11: 710-716.

Megrey, B.A., Rose, K.A., Ito, S., Hay, D.E., Werner, F.E., Yamanaka, Y., and M.N. Aita. 2007. North Pacific basin-scale differences in lower and higher trophic level marine ecosystem responses to climate impacts using a nutrient-phytoplankton–zooplankton model coupled to a fish bioenergetics model. Ecological Modelling, 202: 196-210.

Melillo, J. M., Richmond, T. C. & G.W. Yohe. 2014. Climate Change Impacts in the United States: The Third National Climate Assessment.

Morán X. A., López-Urrutia Á., Calvo-Díaz A., and W.W. Li. 2009. Increasing importance of

small phytoplankton in a warmer ocean, *Global Change Biology*, 16:1137-1144.

Naganuma, T. 1996. Calanoid copepods: linking lower-higher trophic levels by linking lower-higher Reynolds numbers. Marine Ecology Progress Series 136,: 311-313.

Napp, J. M., Incze, L. S., Ortner, P. B., Siefert, D. L. W. & L. Britt. 1996. The plankton of Shelikof Strait, Alaska: Standing stock, production, mesoscale variability and their relevance to larval fish survival. Fisheries Oceanography **5**: 19-38.

Nelson, R. J., Carmack, E. C., McLaughlin, F. A. & G.A. Cooper. 2009. Penetration of Pacific zooplankton into the western Arctic Ocean tracked with molecular population genetics. Marine Ecology Progress Series 381: 129-138.

Ohlberger, J. 2013. Climate warming and ectotherm body size – from individual physiology to community ecology. Functional Ecology 27: 991-1001.

Parmesan, C. & G.A. Yohe. 2003 globally coherent fingerprint of climate change impacts across natural systems. Nature 421: 37-42.

Peter, K. H. & U. Sommer. 2012. Phytoplankton Cell Size: Intra- and Interspecific Effects of

Warming and Grazing. PLoS One 7.

Peter, K. H. & U. Sommer. 2013. Phytoplankton Cell Size Reduction in Response to Warming Mediated by Nutrient Limitation. PLoS One 8.

Peters, R. H. 1983. The ecological implications of body size. Cam- bridge University Press, Cambridge. Putland, J.N., and R.L. Iverson. 2007. Phytoplankton Biomass in a Subtropical Estuary: Distribution, Size Composition, and Carbon:Chlorophyll Ratios. Estuaries and Coasts 30: 878-885.

Rice, E., Dam, H. G. & G. Stewart. 2015. Impact of Climate Change on Estuarine Zooplankton: Surface Water Warming in Long Island Sound Is Associated with Changes in Copepod Size and Community Structure. Estuaries and Coasts 38: 13-23.

Saiz, E., and A. Calbet. 2007. Scaling of feeding in marine calanoid copepods. Limnology and Oceanography 52: 487-921.

Sigler, M.F. et al. 2011. Fluxes, Fins, and Feathers Relationships Among the Bering, Chukchi, and Beaufort Seas in a Time of Climate Change. Oceanography 24: 250-265.

Strasburger, W. W., Hillgruber, N., Pinchuk, A. I. & F.J., Mueter. 2014. Feeding ecology of age-0 walleye pollock (*Gadus chalcogrammus*) and Pacific cod (*Gadus macrocephalus*) in the southeastern Bering Sea. Deep Sea Research Part II: Topical Studies in Oceanography 109: 172-180.

Walther, G.R. et al. 2002 Ecological responses to recent climate change. Nature 416: 389-395.

Wang, M., Overland, J. E. & N.A. Bond. 2010. Climate projections for selected large marine ecosystems. Journal of Marine Systems 79: 258-266.

White, E. P., Ernest, S. K. M., Kerkhoff, A. J. & B.J. Enquist. 2007. Relationships between body size and abundance in ecology. TRENDS in Ecology and Evolution 22: 323-330.

Wilson, M. T., Buchheister, A. & C. Jump. 2011. Regional variation in the annual feeding cycle of juvenile walleye pollock (*Theragra chalcogramma*) in the western Gulf of Alaska. Fishery Bulletin 109: 316-326.

Woodworth-Jefcoats, P.A., Polovina, J.J., and J.C. Drazen. 2017. Climate change is projected to reduce carrying capacity and redistribute species richness in North Pacific pelagic marine

ecosystems. Global Change Biology, 23: 1000–1008.

Yodzis, P., and S. Innes. 1992. Body size and consumer resource dynamics. American Naturalist 139:1151–1175. Yvon-Durocher, G. et al. 2015. Five years of experimental warming increases the biodiversity and productivity of phytoplankton. Public Library of Science Biology 13.

Yvon-Durocher, G., Montoya, J. M., Trimmer, M. & G. Woodward. 2011. Warming alters the size spectrum and shifts the distribution of biomass in freshwater ecosystems. Global Change Biology 17: 1681-1694.